Transcriptomic Changes Triggered by Hypoxia: Evidence for HIF-1α -Independent, [Na$^+$]$_i$/[K$^+$]$_i$-Mediated, Excitation-Transcription Coupling

Svetlana V. Koltsova[1,2], Boris Shilov[3], Julia G. Birulina[4], Olga A. Akimova[1], Mounsif Haloui[2], Leonid V. Kapilevich[4,5], Svetlana V. Gusakova[4], Johanne Tremblay[2], Pavel Hamet[2], Sergei N. Orlov[1,2,4]*

1 Department of Biology, Moscow State University, Moscow, Russia, 2 Department of Medicine, Centre de recherche, Centre hospitalier de l'Université de Montréal, Montreal, Quebec, Canada, 3 Department of Physiology, Pirogov Russian National Research Medical University, Moscow, Russia, 4 Department of Medical Biology, Siberian State Medical University, Tomsk, Russia, 5 Department of Physical Education, Tomsk State University, Tomsk, Russia

Abstract

This study examines the relative impact of canonical hypoxia-inducible factor-1alpha- (HIF-1α and Na$^+$$_i$/K$^+$$_i$-mediated signaling on transcriptomic changes evoked by hypoxia and glucose deprivation. Incubation of RASMC in ischemic conditions resulted in ~3-fold elevation of [Na$^+$]$_i$ and 2-fold reduction of [K$^+$]$_i$. Using global gene expression profiling we found that Na$^+$,K$^+$-ATPase inhibition by ouabain or K$^+$-free medium in rat aortic vascular smooth muscle cells (RASMC) led to the differential expression of dozens of genes whose altered expression was previously detected in cells subjected to hypoxia and ischemia/reperfusion. For further investigations, we selected *Cyp1a1, Fos, Atf3, Klf10, Ptgs2, Nr4a1, Per2* and *Hes1*, i.e. genes possessing the highest increments of expression under sustained Na$^+$,K$^+$-ATPase inhibition and whose implication in the pathogenesis of hypoxia was proved in previous studies. In ouabain-treated RASMC, low-Na$^+$, high-K$^+$ medium abolished amplification of the [Na$^+$]$_i$/[K$^+$]$_i$ ratio as well as the increased expression of all tested genes. In cells subjected to hypoxia and glucose deprivation, dissipation of the transmembrane gradient of Na$^+$ and K$^+$ completely eliminated increment of *Fos, Atf3, Ptgs2* and *Per2* mRNAs and sharply diminished augmentation expression of *Klf10, Edn1, Nr4a1* and *Hes1*. In contrast to low-Na$^+$, high-K$^+$ medium, RASMC transfection with *Hif-1a* siRNA attenuated increments of *Vegfa, Edn1, Klf10* and *Nr4a1* mRNAs triggered by hypoxia but did not impact *Fos, Atf3, Ptgs2* and *Per2* expression. Thus, our investigation demonstrates, for the first time, that Na$^+$$_i$/K$^+$$_i$-mediated, Hif-1α- -independent excitation-transcription coupling contributes to transcriptomic changes evoked in RASMC by hypoxia and glucose deprivation.

Introduction

Hypoxia is characteristic of numerous pathologies, including inflammation [1], cancer [2], obesity [3], systemic and pulmonary hypertension [4;5], atherosclerosis [6] and kidney disease [7]. In 1986, Murry and colleagues reported that the size of myocardial infarcts, arising from 40-min occlusion of the circumplex artery, could be reduced by 75% if the myocardium had been subjected to so-called ischemic preconditioning, i.e., several short occlusions interspersed by periods of reperfusion [8]. Later on, the protective action of brief ischemia was documented in other tissues, including blood vessels [9]. Significantly, the prophylactic influence of ischemic preconditioning was at least partially blocked by inhibitors of RNA synthesis [10;11], suggesting a key role of profound transcriptomic changes documented in global gene expression profiling studies of ischemic tissues [12–18].

Hypoxia-inducible factor 1alpha (HIF-1α), considered to be a major oxygen sensor, regulates gene expression in ischemic tissues via interaction of HIF-1α/HIF-1β heterodimer with hypoxia response elements (HREs) in promoter/enhancer regions of the target gene's DNA. In normoxia, HIF-1α is hydroxylated by oxygen-dependent prolyl hydrolase that elicits its proteasomal degradation. In contrast, under hypoxic conditions, HIF-1α is translocated to the nucleus, where it forms HIF-1α/HIF-1β complex. The list of HIF-1-sensitive genes comprises *Hif-1α per se*, and others related to vasomotor control (nitric oxide synthase-2, adrenomedulin, endothelin-1), angiogenesis (vascular endothelial growth factor (*Vegf*) and its receptor *Flt1*), erythropoiesis and iron metabolism (erythropoietin, transferrin, transferrin receptor, ceruloplasmin), cell proliferation (*Igf1, Igfbp1, Tgfb*), energy metabolism (glucose transporters *Glut1-Glut3*, phosphoenolpyruvate carboxylase, lactate dehydrogenase A, aldose, phosphoglucokinase-1, -L and -C, endolase, tyrosine hydroxylase and plasminogen activator inhibitor-1) (for review see, [10;19-22]).

Immediately after attenuation of oxygen partial pressure and delivery of cell fuels caused by cessation of blood flow, the concentration of ATP and other high-energy phosphate compounds falls, which, in turn, leads to declining ion pump activities, dissipation of electrochemical gradients of K^+, Na^+, Cl^- and Ca^{2+} and plasma membrane depolarization [23]. Numerous research teams reported that $[Ca^{2+}]_i$ elevation triggers cell damage via activation of Ca^{2+}-sensitive isoforms of proteases, protein kinase C, mitogen-activated protein kinase, JNK and p38 as well as transcriptomic alterations evoked by Ca^{2+}_i-sensitive transcriptional elements, such as Ca^{2+}-response elements (CRE), serum-response element (SRE) and activating protein-1 (AP-1) [24]. Post-ischemic reperfusion appears to induce further damage via mitochondrial Ca^{2+} overload and production of reactive oxygen species, including superoxide, hydroxyl, and nitric oxide radicals [25]. Recently, we noted, however, that in several types of mammalian cells Ca^{2+}-depletion increased rather than decreased the number of transcripts whose differential expression was triggered by Na^+,K^+-ATPase inhibition [26]. These data motivate us to propose that, side-by-side with the above-listed signaling pathways, transcriptomic changes in ischemic tissues are evoked by excitation-transcription coupling via a novel Na^+_i/K^+_i-mediated, Ca^{2+}_i-independent mechanism. We designed the present study to examine this hypothesis.

Results

Effect of ouabain, K+-free medium and hypoxia on intracellular content of monovalent ions and ATP

Six-hr inhibition of Na^+,K^+-ATPase in RASMC by ouabain increased $[Na^+]_i$ from 15–20 to 130 mM and decreased $[K^+]_i$ from ~150 to 25 mM (Fig. 1). Somewhat similar elevation of the $[Na^+]_i/[K^+]_i$ ratio was detected with 6 hr of Na^+,K^+-ATPase inhibition in K^+-free medium. Dissipation of the transmembrane gradients of monovalent cations, triggered by ouabain and K^+-free

medium, was accompanied by elevation of $[Cl^-]_i$ from ~40 to 80 and 60 mM, respectively (Fig. 1).

Figure 2 shows that 24-hr incubation of RASMC in hypoxia and glucose starvation decreased intracellular ATP content by ~3-fold whereas ouabain attenuated this parameter by less than 20%. The actions of hypoxia and ouabain on ATP content were preserved in low-Na^+, high-K^+ medium. Treatment with ouabain resulted in almost 10-fold gain of $[Na^+]_i$ and virtually similar loss of $[K^+]_i$. In hypoxic conditions, $[Na^+]_i$ and $[K^+]_i$ were increased and decreased by 3- and 2-fold, respectively. As predicted, dissipation of the transmembrane gradients of monovalent cations in low-Na^+, high-K^+ medium almost completely abolished the actions of ouabain and hypoxia on the $[Na^+]_i/[K^+]_i$ ratio (Fig. 2). Viewed collectively, these results allowed us to hypothesize that transcriptomics changes triggered by hypoxia are at least partially caused by Na^+_i/K^+_i-mediated excitation-transcription coupling discovered in our recent studies [26]. Data considered below support this hypothesis.

Identification and functional characterization of $[Na^+]_i/]K^+]_i$-sensitive transcriptome in RASMC

Affymetrix data from 3 independent experiments were normalized and analyzed by PCA [27]. Each point on PCA represents the gene expression profile of an individual sample. Samples that are near each other in the resulting 3-dimensional plot have a similar transcriptome while those that are further apart have dissimilar transcriptional profiles. This approach identified ouabain and K^+-free medium as major sources of variability within datasets (Fig. 3A).

Figure 3B discloses that the number of differentially-expressed transcripts in RASMC treated for 6 hr with ouabain or K^+-free medium totalled 8,266 and 8,264, respectively. Further analysis determined that the expression of 6,412 transcripts was affected by both stimuli (Fig. 3B). Significantly, we observed highly significant $(p<4\times10^{-9})$ and positive $(R^2>0.80)$ correlations between levels of differentially-expressed transcripts identified in the presence of
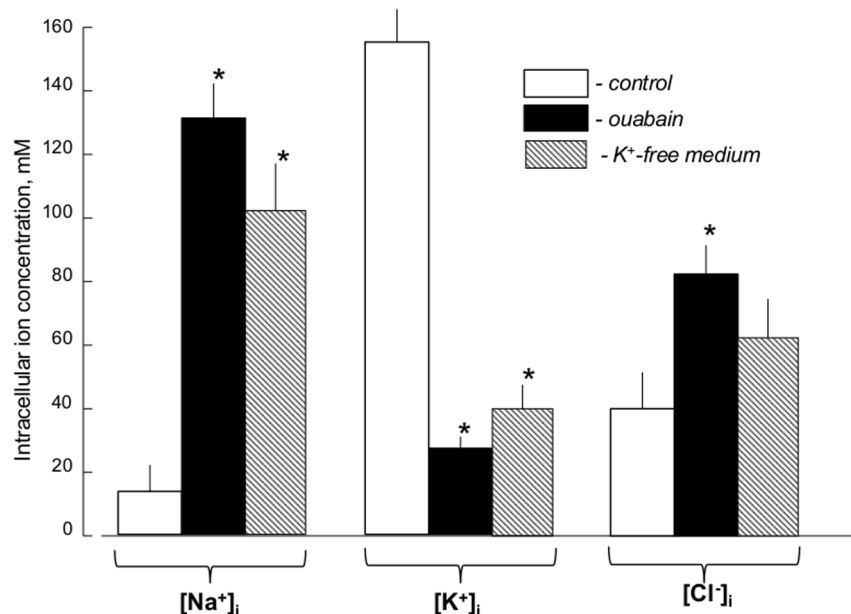

Figure 1. Effect of Na^+,K^+-ATPase inhibition on the intracellular content of monovalent ions. RASMC were incubated in control and K^+-free medium or in the presence of 3 mM ouabain for 6 hr. Means ± S.E. from 3 independent experiments performed in quadruplicate are shown. *p<0.05 compared to controls.
doi:10.1371/journal.pone.0110597.g001
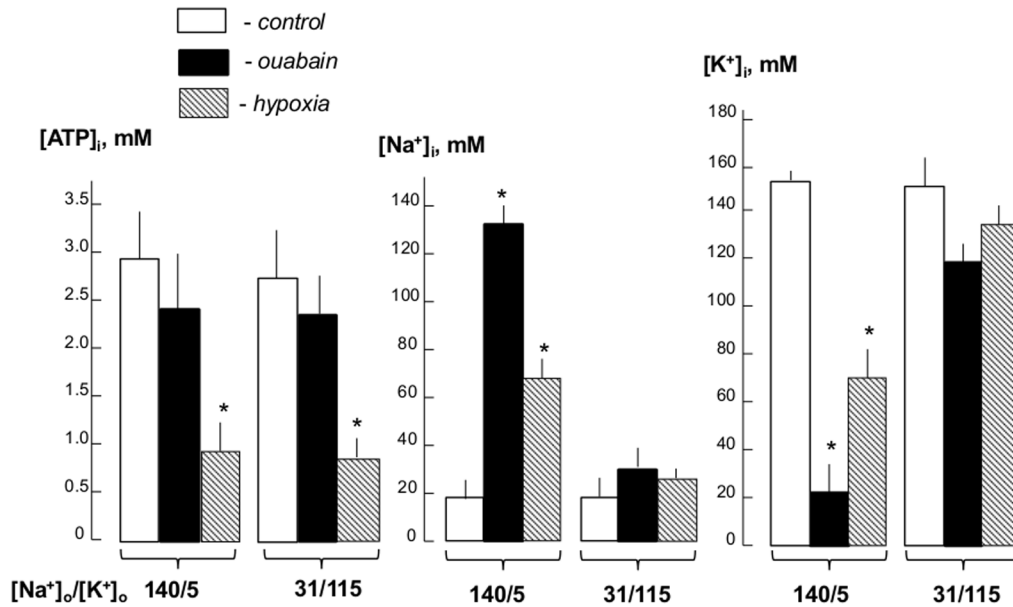
Figure 2. Effect of ouabain and hypoxia on intracellular Na⁺, K⁺ and ATP concentrations. RASMC were incubated for 24 hr under normal oxygen partial pressure (5% CO_2/air - *control*) ± 3 μM ouabain or exposure to hypoxia (5% CO_2/95% N_2)/glucose deprivation in normal high-Na⁺, low-K⁺ ($[Na^+]_o/[K^+]_o = 140/5$) or in low-Na⁺, high-K⁺ DMEM-like medium ($[Na^+]_o/[K^+]_o = 131/115$). Means $\pm$ S.E. from 3 independent experiments performed in quadruplicate are shown. *$p < 0.05$ compared to the controls.
doi:10.1371/journal.pone.0110597.g002

ouabain and K⁺-free medium (Fig. 4). Because the gain of $[Na^+]_i$ and loss of $[K^+]_i$ in cells treated with ouabain or K⁺-free medium are similar (Fig. 1), the results strongly suggest that the changes in

gene expression evoked by both stimuli occur in response to elevation of the $[Na^+]_i/[K^+]_i$ ratio rather than $[Na^+]_i/[K^+]_i$-independent events.
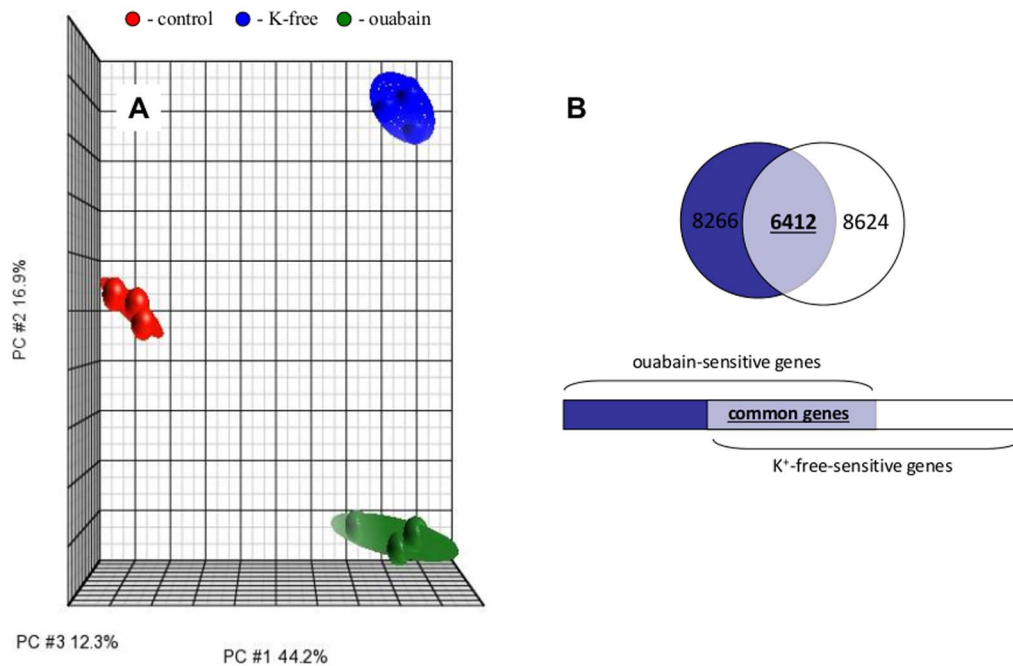
Figure 3. Effect of Na⁺,K⁺-ATPase inhibition on the RASMC transcriptome. Cells were incubated for 6 hr in control DMEM, K⁺-free DMEM or DMEM containing 3 mM ouabain. All experiments are repeated 3 times. **A**. PCA of transcriptomic changes. Ellipsoids highlight portioning of samples based on type of treatment. The principal components in 3-dimensional graphs (PC#1, PC#2 and PC#3) represent the variability of gene expression level within datasets. **B**. Comparative analysis of the impact of Na⁺,K⁺-ATPase inhibition by ouabain and K⁺-free medium on the RASMC transcriptome. The total number of genes whose expression is altered by ouabain and K⁺-free medium by more than 1.2-fold with $p < 0.05$ is indicated; the number of genes affected by both stimuli appears in **bold**.
doi:10.1371/journal.pone.0110597.g003
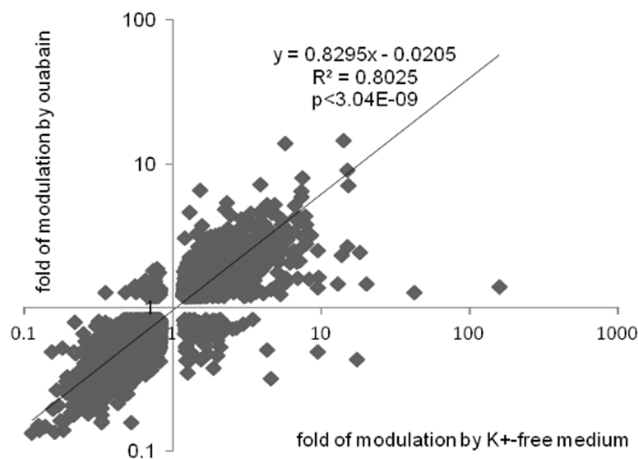
Figure 4. Correlation analysis of transcripts whose expression is altered by ouabain and K⁺-free medium in RVSMC by more than by 1.2-fold with p<0.05. The total number of transcripts subjected to analysis is shown in Figure 2B. Transcript expression in control cells was taken as 1.00. The fold change was determined as log transformed treatment/control expression ratio.
doi:10.1371/journal.pone.0110597.g004

It should be noted that, together with increment of the $[Na^+]_i/[K^+]_i$ ratio, ouabain and K⁺-free medium may affect cells independently of suppression of Na^+,K^+-ATPase-mediated ion fluxes. Thus, recent studies revealed that ouabain triggered interaction of the Na^+,K^+-ATPase α-subunit with the membrane-associated nonreceptor tyrosine kinase Src, activation of Ras/Raf/ERK1,2, phosphatidyl inositol 3-kinase (PI(3)K), PI(3)K-dependent protein kinase B, phospholipase C, $[Ca^{2+}]_i$ oscillations and augmented production of ROS (for review, see [28;29]). On the other hand, transfer of highly K⁺-permeable cells to K⁺-free medium results in transient membrane hyperpolarization that has a tissue-specific impact on the activity of diverse voltage-sensitive, membrane-bound proteins [30;31] and the distribution of other permeable ions, including Cl⁻ (Fig. 1). Indeed, we noted that the expression of several genes detected, such as *Cxcl2, Cxcl5, Tnfs5, Lif* and *Vcam1*, is sharply increased in K⁺-free medium compared to ouabain-treated cells (Table 1). This considered, we focused our analysis on $[Na^+]_i/[K^+]_i$-sensitive genes whose expression in K⁺-free medium and in the presence of ouabain was less than 2-fold different. $[Na^+]_i/[K^+]_i$-sensitive genes, whose expression was increased or decreased by more that 3-fold, are listed in Tables 2 and 3, respectively.

Although functional characterization is somewhat artificial – because genes are usually multifunctional and fall into several categories – we ascertained that both up- and down-regulated $[Na^+]_i/[K^+]_i$-sensitive transcriptomes were enriched with genes involved in transcription/translation, cell adhesion, migration, proliferation, differentiation and death (Tables 1 and 2, Fig. 5). We also noted that, among $[Na^+]_i/[K^+]_i$-sensitive genes, the relative content of transcription/translation regulators was ∼3–4-fold higher than in total mammalian genomes [32]. Keeping this in mind, we undertook an additional search for genes encoding HIF-1, AP-1, cyclic AMP response element-binding protein (CREB), nuclear factor kappa-B (NFκB), early growth response factors (EGR), i.e. major transcription factors involved in transcriptomic changes evoked by hypoxia (for review, see [33]). Table 3 demonstrates that Na^+,K^+-ATPase inhibition resulted in augmented expression of genes encoding AP-1 and *Egr1* and down-regulation of genes encoding regulators of the NFkB- and

p53-mediated signalling pathways. We found less than 2-fold elevation of *Sp1, Creb1* and *Creb5* and lack of any impact of increment of the $[Na^+]_i/[K^+]_i$ ratio on the transcription of other hypoxia-inducible transcription factors: *Hif-1a, Hif-1b, Hif-2a, Hif-3a, p65, cRel, RelB, p50, p52, IκB, p53, Sp3, Gata2, Stat5, Gadd153*.

In silico search for subset of genes whose expression is affected both elevation of the $[Na^+]_i/]K^+]_i$ ratio and hypoxia

To select candidate genes for the investigation of relative impact of HIF-1α- and $[Na^+]_i/[K^+]_i$-mediated signaling triggered by hypoxia, we performed a comparative analysis of our results on the identification of $[Na^+]_i/]K^+]_i$-sensitive in RASMC and PubMed database for genes affected by hypoxia/ischemia. In Tables 1 and 2, $[Na^+]_i/]K^+]_i$-sensitive transcripts found in PubMed database as genes affected by hypoxia and/or ischemia are shown in **bold** with number of publications given in parentheses. Then, we performed and additional search $[Na^+]_i/]K^+]_i$- and hypoxia-sensitive genes in manuscripts investigated transcriptomic changes triggered by hypoxia/ischemia using the global gene expression profiling technology [12-14;16;17]. $[Na^+]_i/]K^+]_i$-sensitive genes found in these papers are *italicized* in Tables 1 and 2. These two approaches led us to conclusion that relative percentages of hypoxia-sensitive genes among up- and down-regulated $[Na^+]_i/[K^+]_i$-sensitive genes were ∼40% and 12%, respectively, i.e. much higher than predicted from random distribution in the rat genome of 280 $[Na^+]_i/[K^+]_i$-sensitive genes and 60 hypoxia-sensitive genes annotated in Tables 1 and 2.

Role of HIF-1α- and $[Na^+]_i/[K^+]_i$-mediated signaling

For further investigations, we selected *Cyp1a1, Fos, Atf3, Klf10, Ptgs2, Nr4a1, Per2* and *Hes1*, i.e. genes possessing the highest increments of expression under sustained Na^+,K^+-ATPase inhibition and whose implication in the pathogenesis of hypoxia was proved in previous studies. Thus, FOS and ATF3, together with JUN, form dimeric transcription factor AP-1 whose augmented expression was documented in all types of cells subjected to hypoxia [33]. *Ptgs2* encodes an inducible isoform of cyclooxygenase-2 (COX-2) whose role in the pathophysiology of hypoxia is well-documented [34]. *Klf10* is a Kruppel-like zinc-finger transcription factor family member involved in hypoxia-dependent angiogenesis via COX-1 activation [35]. Nerve growth factor IB, also known as *Nur77* or *Nr4a1*, is the nuclear receptor of transcription factors stabilizing HIF-1α, which increases its transcriptional activity [36]. *Hes1* is the basic helix-loop-helix transcription factor whose expression is sharply augmented after ischemic renal failure [37]. The core circadian oscillator is composed of a transcription-translation feedback loop in which *Clock* and *Bmal1* are positive regulators, and *Per1, Per2, Cry1* and *Cry2* act as negative regulators [38]. It has been shown that *Per2* promotes circadian stabilization of HIF-1α activity that is critical for myocardial adaptation to ischemia [39;40]. *Cyp1a1* encodes a cytochrome P450 family member and its expression is mediated by HIF-1β [44]. Vascular endothelial growth factor (*Vegfa*) and endothelin (*Edn1*) were chosen as positive controls for canonical HIF-1α-sensitive genes.

To examine the relative impact of HIF-1α-mediated and $[Na^+]_i/[K^+]_i$-dependent signaling, we compared the effects of hypoxia and ouabain on expression of the above-listed selected genes in control high-Na⁺, low-K⁺ medium, after dissipation of the transmembrane gradients of monovalent cations in high-K⁺, low-Na⁺ medium and in cells transfected with *Hif-1a* siRNA. As

Table 1. Genes whose expression was increased in RASMC subjected to Na⁺,K⁺-ATPase inhibition.

Gene symbol//gene title (ref #) – functional categories	K⁺-free medium		ouabain	
	Fold change	p value	Fold change	p value
Gdf15//growth differentiation factor 15 (D) - D	15.17	1.88E-06	7.44	6.03E-06
Ereg//epiregulin (1) – D	**15.14**	**1.59E-06**	**9.63**	**4.10E-06**
Cyp1a1//cytochrome P450, family 1, subfamily a (15) - O	**14.22**	**1.59E-06**	**15.58**	**2.95E-06**
Fos//FBJ osteosarcoma oncogene (427) – T	**7.91**	**2.23E-05**	**3.95**	**1.23E-04**
Atf3//activating transcription factor (27) – T	**7.83**	**2.85E-05**	**4.53**	**1.07E-04**
Slc9a3//solute carrier family 9 (sodium/hydrogen exchang – O	7.52	2.13E-06	3.25	1.22E-05
Nppc//natriuretic peptide C – O	7.42	6.35E-06	6.80	9.53E-06
Bhlhe41//basic helix-loop-helix family, member e41 – T	7.42	6.59E-06	6.23	1.13E-05
Klf10//Kruppel-like factor 10 (2) – T	**7.16**	**4.32E-06**	**4.09**	**1.38E-05**
Trib1//Tribbles homolog 1 (Drosophila) (2) – D	**7.09**	**1.50E-06**	**4.47**	**4.54E-06**
Il6r//interleukin 6 receptor (1) – I	**6.71**	**9.08E-07**	**4.37**	**3.17E-06**
Ets2//v-ets erythroblastosis virus E26 oncogene homolog 2– T	*6.68*	*4.93E-06*	*5.35*	*9.09E-06*
Fam43a//family with sequence similarity 43, member A – U	6.56	6.89E-06	3.45	3.34E-05
Arrdc4//arrestin domain containing 4– U	5.89	1.70E-06	3.06	7.44E-06
Tppp//tubulin polymerization promoting protein – D	5.89	1.11E-05	3.58	4.18E-05
Ptgs2//prostaglandin-endoperoxide synthase 2 (588) – I	**5.68**	**1.44E-06**	**3.71**	**4.45E-06**
F3//coagulation factor III (thromboplastin, tissue factor I	*5.64*	*1.62E-06*	*3.39*	*5.50E-06*
Enc1//ectodermal-neural cortex – D	5.61	9.08E-07	3.85	2.57E-06
Mmp28//matrix metallopeptidase 28– I	*5.47*	*3.64E-06*	*4.24*	*7.44E-06*
Epha2//Eph receptor A2 (3) – D	**5.46**	**2.73E-06**	**3.32**	**8.72E-06**
RGD1307396//similar to RIKEN cDNA 6330406I15 – U	5.39	2.12E-06	3.94	5.19E-06
Slc25a25//solute carrier family 25 (mitochondrial Pi carrier) – O	5.04	2.66E-06	2.85	1.12E-05
Nr4a1//nuclear receptor subfamily 4, group A (14) – T	**4.99**	**9.44E-06**	**4.67**	**1.33E-05**
Per2//period homolog 2 (Drosophila) (6) – O	**4.88**	**7.48E-06**	**5.47**	**8.33E-06**
Zbtb2//zinc finger and BTB domain containing 2– T	4.68	2.63E-06	3.09	8.01E-06
Rab32//RAB32, member RAS oncogene family – T	*4.68*	*1.49E-06*	*2.51*	*7.26E-06*
Isg20//interferon stimulated exonuclease gene 20– I	*4.67*	*2.44E-06*	*4.71*	*4.06E-06*
Hbegf//heparin-binding EGF-like growth factor (4) – D	**4.65**	**2.60E-06**	**2.69**	**1.10E-05**
Pde4b//phosphodiesterase 4B, cAMP-specific – O	*4.52*	*3.64E-06*	*2.43*	*2.15E-05*
Csrnp1//cysteine-serine-rich nuclear protein 1–D	4.52	3.63E-06	3.52	7.73E-06
PVR//poliovirus receptor - D	4.50	3.47E-06	3.58	7.26E-06
Hes1//hairy and enhancer of split 1 (Drosophila) (34) – T	**4.47**	**5.68E-06**	**2.94**	**1.93E-05**
Bcl6//B-cell CLL/lymphoma 6 (1) –D	**4.45**	**2.12E-06**	**2.90**	**7.26E-06**
Ier5//immediate early response 5-T	*4.45*	*5.59E-06*	*2.76*	*2.26E-05*
Sgk1//serum/glucocorticoid regulated kinase 1 (14) - O	**4.42**	**3.96E-06**	**3.64**	**7.69E-06**
Plk3//polo-like kinase 3 (20) -D	**4.41**	**1.03E-05**	**3.13**	**3.05E-05**
Klf5//Kruppel-like factor 5-T	*4.39*	*1.17E-05*	*3.43*	*2.64E-05*
Mthfd2l//methylenetetrahydrofolate dehydrogenase – O	4.38	9.85E-06	2.49	6.04E-05
Areg//amphiregulin (3) – D	**4.37**	**1.00E-05**	**3.26**	**2.51E-05**
RGD1563891//similar to core 2 beta-1,6-N-acetylglucosam – U	4.36	5.54E-05	3.52	1.17E-04
Fst//follistatin (9) – D	**4.35**	**6.59E-06**	**5.50**	**6.34E-06**
Fosl1//fos-like antigen 1-T	*4.27*	*1.20E-05*	*3.41*	*2.59E-05*
Ier2//immediate early response 2 (1) – T	**4.24**	**2.62E-05**	**1.99**	**6.15E-04**
Baiap2//BAI1-associated protein 2-D	4.14	9.08E-07	3.98	2.57E-06
Rassf9//Ras association (RalGDS/AF-6) domain family – D	4.12	2.41E-06	2.86	7.26E-06
Chka//choline kinase alpha – O	4.10	1.82E-06	4.71	2.95E-06
Irf2bpl//interferon regulatory factor 2-binding protein-like – I	*4.10*	*3.37E-05*	*3.27*	*7.69E-05*
Mum1l1//melanoma-associated antigen (mutated) 1-like 1–I	*4.00*	*4.60E-06*	*2.69*	*1.53E-05*

Table 1. Cont.

Gene symbol//gene title (ref #) – functional categories	K+-free medium		ouabain	
	Fold change	p value	Fold change	p value
Nr4a3//nuclear receptor subfamily 4, group A, mem 3 (5) – T	**3.99**	**1.00E-05**	**4.13**	**1.19E-05**
Tas2r135//taste receptor, type 2, member 135–O	3.94	3.86E-05	3.56	6.11E-05
Errfi1//ERBB receptor feedback inhibitor 1–D	3.93	4.30E-06	2.82	1.19E-05
Skil//SKI-like oncogene - T	3.92	9.08E-07	2.13	6.03E-06
Zswim4//zinc finger, SWIM-type containing 4–T	3.92	2.09E-06	2.31	1.02E-05
Dusp10//dual specificity phosphatase 10 (3)-D	**3.92**	**8.95E-06**	**2.09**	**8.82E-05**
Has2//hyaluronan synthase 2 (3) –I	**3.91**	**9.85E-06**	**7.60**	**4.67E-06**
Txnip//thioredoxin interacting protein (9) – I	**3.88**	**1.82E-06**	**2.31**	**8.58E-06**
Mdm2//Mdm2 p53 binding protein homolog (mouse) (22) – T	**3.85**	**9.08E-07**	**2.98**	**2.95E-06**
Fam171b//family with sequence similarity 171, member B – U	3.84	3.05E-06	4.82	3.26E-06
Stk17b//serine/threonine kinase 17b –O	3.76	3.65E-06	4.00	4.67E-06
Zfp36//zinc finger protein 36–T	*3.70*	*6.56E-05*	*2.15*	*7.25E-04*
Rab20//RAB20, member RAS oncogene family –I	3.66	4.53E-06	3.90	5.52E-06
Pnrc1//proline-rich nuclear receptor coactivator 1–T	3.66	2.19E-07	3.10	7.72E-07
Abcb1b//ATP-binding cassette, subfamily B, mem 1B (3) – O	**3.65**	**9.08E-07**	**2.72**	**3.17E-06**
Smad3//SMAD family member 3 (20) –T	**3.64**	**4.27E-06**	**2.78**	**1.04E-05**
RGD1306119//similar to transcriptional regulating prot 132 – T	3.59	1.13E-05	1.80	2.42E-04
Htr2a//5-hydroxytryptamine (serotonin) receptor 2A (1) – O	**3.58**	**9.08E-07**	**3.10**	**2.78E-06**
Jun//jun proto-oncogene (799) –T	**3.57**	**1.77E-06**	**2.76**	**4.54E-06**
Zfat//zinc finger and AT hook domain containing – T	3.57	4.59E-06	3.01	8.69E-06
Dusp6//dual specificity phosphatase 6 (2) -O	**3.56**	**4.79E-06**	**2.42**	**1.73E-05**
Ier5l//immediate early response 5-like T	3.55	4.98E-06	2.71	1.29E-05
Bmp2//bone morphogenetic protein 2 (13) –D	**3.52**	**3.96E-05**	**3.69**	**4.14E-05**
Gnat1//guanine nucleotide-binding protein, alpha t –O	3.50	2.44E-06	3.86	3.26E-06
RGD1305254//similar to transmembrane protein 2–U	3.48	3.31E-05	2.14	2.69E-04
Alkbh//alkB, alkylation repair homolog (E. coli) –D	3.45	2.26E-06	2.44	7.40E-06
Klf4//Kruppel-like factor 4 (gut) (5) –T	**3.44**	**1.54E-05**	**2.49**	**5.57E-05**
Hapln3//hyaluronan and proteoglycan link protein 3 – O	3.44	2.58E-05	1.95	3.45E-04
Mafk//v-maf musculoaponeurotic fibrosarcoma onco hom K–T	*3.42*	*8.48E-06*	*2.75*	*1.91E-05*
Maff//v-maf musculoaponeurotic fibrosarcoma onco hom F-T	*3.42*	*2.09E-05*	*2.55*	*6.83E-05*
Dusp16//dual specificity phosphatase 16 (2) –O	**3.39**	**1.94E-05**	**2.23**	**1.10E-04**
Gprc5a//G protein-coupled receptor, family C, gr 5, mem A–O	3.38	3.26E-05	4.73	1.74E-05
Lgr5//leucine-rich repeat contain G protein coupled recept –O	3.32	1.11E-05	4.12	8.86E-06
Per1//period homolog 1 (Drosophila) (4) –O	**3.32**	**5.54E-06**	**4.09**	**5.06E-06**
Cd80//Cd80 molecule (28) –I	**3.30**	**6.40E-06**	**2.10**	**3.72E-05**
Mybl1//myeloblastosis oncogene-like 1 (1) –T	**3.29**	**1.86E-05**	**2.03**	**1.55E-04**
Pim1//pim-1 oncogene (5) –D	**3.27**	**6.86E-06**	**1.84**	**8.03E-05**
Osmr//oncostatin M receptor –I	3.25	2.76E-05	2.00	2.57E-04
Smad7//SMAD family member 7 (6) –D	**3.23**	**4.22E-06**	**2.05**	**2.23E-05**
Cpeb4//cytoplasmic polyadenyl element bind prot 4 (1) –T	**3.20**	**4.79E-06**	**3.01**	**7.42E-06**
Aen//apoptosis-enhancing nuclease (5) D	**3.17**	**5.96E-06**	**3.10**	**8.39E-06**
Nr4a2//nuclear receptor subfamily 4, group A, mem 2 (4) – T	**3.16**	**1.56E-05**	**3.99**	**1.15E-05**
Tnfrsf1b//tumor necrosis factor receptor superfamily –D	**3.15**	**2.67E-05**	**1.99**	**2.31E-04**
Lhfpl2//lipoma HMGIC fusion partner-like 2–O	3.10	4.60E-06	1.76	5.10E-05
Rap2b//RAP2B, member of RAS oncogene family –O	3.07	1.00E-05	2.34	3.03E-05
Lmbrd2//LMBR1 domain containing 2–U	3.07	9.85E-06	2.70	1.77E-05
Cdc42ep1//CDC42 effector protein (Rho GTPase binding) 1 – D	3.06	2.92E-05	2.80	4.71E-05
Kdm6b//lysine (K)-specific demethylase 6B –T	3.04	7.50E-06	2.04	3.94E-05

Table 1. Cont.

Gene symbol//gene title (ref #) – functional categories	K⁺-free medium		ouabain	
	Fold change	p value	Fold change	p value
RGD1310794//similar to RIKEN cDNA C030048B08 - D	3.04	2.47E-04	4.01	1.07E-04
Sertad2//SERTA domain containing 2-T	*3.03*	*1.40E-05*	*2.55*	*3.05E-05*

RASMC were treated with 3 mM ouabain or K⁺-free medium for 6 hr. Listed are assigned genes whose expression was increased in K⁺-free medium by more than 3-fold and was different by less than 2-fold in the presence of ouabain compared to K⁺-free medium. GeneChip expression analysis was performed as described in the Methods section. mRNA content in control cells was taken as 1.00. Genes whose expression is altered in ischemia/hypoxia are shown **in bold**. Appearing in parentheses are numbers of citations in PubMed. Listed *in italics* are genes whose differential expression was detected in ischemic tissue by whole genome microarray-based analysis [12–18]. Data on gene function from GeneCards database (www.genecards.org) were used for identification of gene function. Functional categories: T– regulators of transcription/translation, RNA processing and degradation; D– regulators of cell adhesion, migration, proliferation, differentiation and death; I– inflammation and immune responses; O– others; U– unknown function.
doi:10.1371/journal.pone.0110597.t001

demonstrated in other cell types studied so far [22;41], hypoxia slightly augmented *Hif-1a* mRNA (Table 4) and increased immunoreactive HIF-1α protein content by ∼5-fold (Fig. 6). RASMC transfection with *Hif-1a* siRNA but not with scrambled siRNA decreased *Hif-1a* expression by ∼3-fold and sharply attenuated the rise in HIF-1α protein triggered by hypoxia (Fig. 6). Ouabain increased baseline *Hif-1a* mRNA by ∼50% (Table 4) and slightly curbed HIF-1α protein content (Fig. 6). Confirming previous observations [10], hypoxia increased *Vegfa* and *Edn1* mRNA content by 12- and 4-fold, respectively (Table 5). Transfection with *Hif-1a* siRNA decreased hypoxia-dependent increments of *Vegfa* and *Edn1* mRNA by ∼4- and 2-fold, respectively (Fig. 6). Ouabain did not significantly affect *Vegfa* and augmented *Edn1* mRNA by 2.5-fold. Dissipation of the transmembrane gradients of monovalent cations in low-Na⁺, high-K⁺ medium did not alter the expression of *Vegfa* triggered by hypoxia and decreased *Edn1* mRNA by 2-fold. Viewed collectively, these data strongly support the efficacy of Hif1α-siRNA function.

Dissipation of the transmembrane gradients of monovalent cations completely suppressed increments of *Fos, Atf3, Ptgs2* and *Per2* mRNA and sharply diminished elevations of *Klf10, Edn1, Nr4a1* and *Hes1* expression seen in hypoxic conditions (Fig. 7). Consistent with data obtained in other cell types, including human VSMC [42;43], hypoxia increased *Fos, Atf3, Klf10, Ptgs2, Nr4a2, Per2* and *Hes1* expression from 2- to 6-fold (Fig. 7). Transfection with *Hif-1a* siRNA decreased *Klf10* and *Nr4a* mRNA increments evoked by hypoxia by ∼2-fold but did not affect hypoxia-induced *Fos, Atf3, Ptgs2* and *Per2* expression. In contrast to the other genes listed in Table 4, hypoxia decreased *Cyp1a1* mRNA by 2-fold in concordance with attenuated *Cyp1a1* expression in the human microvasculature subjected to hypoxia [44]. The expression of all 8 tested genes was heightened from 3- to 10-fold in the presence of ouabain. These increments were completely abolished under dissipation of the transmembrane gradients of monovalent cations in low-Na⁺, high-K⁺ medium. In contrast to low-Na⁺, high-K⁺ medium, transfection with *Hif-1a* siRNA did not affect the expression of these genes in ouabain-treated RASMC (Table 4). Dissipation of the transmembrane gradient of monovalent cations completely inhibited increments of *Fos, Atf3, Ptgs2* and *Per2* mRNA and sharply diminished elevation of *Klf10, Edn1, Nr4a1* and *Hes1* expression seen in hypoxic conditions (Fig. 7).

Localization of (A/G)CGTG hypoxia response elements within 5′-UTR

Several research teams reported that HIF-1α regulates gene expression in ischemic tissues via interaction of HIF-1α/HIF-1β heterodimer with HREs containing (A/G)CGTG consensus in promoter/enhancer regions of the target gene's DNA such as VEGFA [45] and EDN1 [46]. Considering this, we employed SCOPE service (Suite for Computational Identification of Promoter Elements): http://genie.dartmouth.edu/scope/[47] for the search of (A/G)CGTG consensus within 5′-untranslated regions (5′-UTR) of [Na⁺]$_i$/[K⁺]$_i$-sensitive genes listed in Table 4. Using this approach we found numerous (A/G)CGTG sequences within 5′-UTR encoding canonical HIF-1-sensitve genes (*Edn1* and *Vegfa*) as well as all [Na⁺]$_i$/[K⁺]$_i$-sensitive genes listed in Table 4. Importantly, we failed to find any fixed position for this consensus within 10,000 bp 5′-UTRs of HIF1α-sensitive vs HIF1α-resistant genes (Fig. 8). Moreover, we observed that in several [Na⁺]$_i$/[K⁺]$_i$-sensitive genes proximal 1,500 bp segments of 5′-UTRs are more abundant with (A/G)CGTG sequence as compared to canonical HIF-sensitive transcripts (Fig. 9). Thus, 1,500 bp 5′-UTRs of *Atf3* and *Edn1* contains 8 and 3 (A/G)CGTG sequences. This observation is also confirmed by Sig Value parameter having a value of 28.4 for 1500 bp 5′-UTRs of genes listed in Table 5. If the search is not restricted to positions of 1500 bp, Sig Value is negative indicating the absence of predictive capabilities for the consensus sequence.

Discussion

HIF-1α the sole known oxygen sensor, regulates gene expression in ischemic tissues via interaction of HIF-1α/HIF-1β heterodimer with HREs in promoter/enhancer regions of the target gene's DNA [19–22]. Our investigation demonstrates, for the first time, that [Na⁺]$_i$/[K⁺]$_i$-sensitive excitation-transcription coupling contributes to the transcriptomic changes triggered by hypoxia independently of HIF-1α-mediated signaling. Evidences supporting this conclusion are listed below.

First, elevation of the [Na⁺]$_i$/[K⁺]$_i$ ratio evoked by 6-hr inhibition of Na⁺,K⁺-ATPase by ouabain or K⁺-free medium resulted in differential expression of more than 6,000 transcripts (Fig. 3). The list of [Na⁺]$_i$/[K⁺]$_i$-sensitive genes whose expression changed by more than 3-fold (Tables 1 and 2) is abundant with genes whose differential expression was reported to be affected by hypoxia or ischemia/reperfusion.

Table 2. Genes whose expression was decreased in RASMC subjected to Na$^+$,K$^+$-ATPase inhibition.

Gene symbol//gene title (ref #) – functional categories	K$^+$-free medium		ouabain	
	Fold change	p value	Fold change	p value
Syt17//synaptotagmin XVII -O	−3.01	1.19E-05	−1.81	1.35E-04
Phyh//phytanoyl-CoA 2-hydroxylase –O	−3.02	4.62E-05	−2.84	6.80E-05
Ttc21b//tetratricopeptide repeat domain 21B –O	−3.03	4.28E-05	−4.06	2.24E-05
Parp2//poly (ADP-ribose) polymerase 2–T	−3.03	2.91E-05	−3.94	1.77E-05
RGD1309534//similar to RIKEN cDNA 4931406C07 –U	−3.03	2.51E-05	−2.12	1.31E-04
Mus81//MUS81 endonuclease homolog (S. cerevisiae) – T	−3.03	8.76E-06	−2.52	1.88E-05
Lactb2//lactamase, beta 2–O	−3.04	2.89E-05	−3.41	2.48E-05
Fbxw17//F-box and WD-40 domain protein 17-U	−3.05	3.50E-05	−3.61	2.57E-05
Gnb5//guanine nucleotide binding prot beta 5 (1) – O	**−3.05**	**1.03E-05**	**−2.63**	**2.03E-05**
Mrpl32//mitochondrial ribosomal protein L32 –O	−3.06	5.76E-05	−1.83	8.71E-04
MGC94199//similar to RIKEN cDNA 2610301B20; -U	−3.06	2.15E-04	−3.68	1.26E-04
Zscan12//zinc finger and SCAN domain containing 12–T	−3.07	2.82E-05	−3.37	2.57E-05
Top3b//topoisomerase (DNA) III beta –T	−3.07	9.85E-06	−3.90	7.40E-06
Zfp259//zinc finger protein 25 –T	*−3.08*	*3.32E-06*	*−1.61*	*5.70E-05*
Myo19//myosin XIX –O	−3.09	1.64E-05	−2.24	6.71E-05
Prkag1//protein kinase, AMP-activat, gamma 1 (1) –O	**−3.09**	**4.04E-06**	**−1.67**	**6.07E-05**
Gtpbp5//GTP-binding protein 5–T	−3.10	2.84E-05	−2.83	4.59E-05
Dcaf4//DDB1 and CUL4 associated factor 4–O	−3.10	1.20E-05	−2.59	2.64E-05
LOC687284//similar to excision repair cross-compl –U	−3.10	7.20E-06	−3.34	8.30E-06
Gdf10//growth differentiation factor 10–D	*−3.11*	*9.18E-05*	*−2.69*	*1.83E-04*
Tmem184c//transmembrane protein 184C –D	−3.11	3.45E-06	−2.02	1.69E-05
Deadc1//deaminase domain containing 1–O	−3.11	4.60E-05	−3.13	5.42E-05
RGD1311422//similar to CG8841-PA –U	−3.12	9.85E-06	−2.60	2.07E-05
Parp1//poly (ADP-ribose) polymerase 1 (46) –D	**−3.13**	**1.87E-06**	**−2.75**	**4.29E-06**
Rtel1//regulator of telomere elongation helicase 1 –D	−3.13	8.33E-06	−2.29	2.80E-05
Dhcr7//7-dehydrocholesterol reductase –O	−3.14	3.83E-05	−4.86	1.54E-05
Gatsl2//GATS protein-like 2–T	−3.14	3.51E-05	−1.97	3.31E-04
Glb1l2//galactosidase, beta 1-like 2–O	−3.14	2.49E-05	−3.60	2.09E-05
RGD1563798//similar to BC040823 protein –U	−3.14	2.24E-05	−2.88	3.62E-05
Gbas//glioblastoma amplified sequence –O	−3.15	2.23E-06	−2.92	4.31E-06
Cybasc3//cytochrome b, ascorbate dependent 3–O	*−3.15*	*4.82E-06*	*−3.72*	*4.97E-06*
Fn3krp//fructosamine-3-kinase-related protein –O	−3.16	2.94E-06	−3.92	3.24E-06
Mrpl34//mitochondrial ribosomal protein L34 –T	−3.17	3.78E-04	−2.27	1.88E-03
Nsun6//NOP2/Sun domain family, member 6–U	−3.17	1.49E-05	−1.99	1.19E-04
Zdhhc12//zinc finger, DHHC-type containing 12–T	−3.17	5.52E-05	−4.22	2.93E-05
Rabl5//RAB, member RAS oncogene family-like 5–U	−3.18	5.97E-05	−2.89	9.60E-05
Aacs//acetoacetyl-CoA synthetase –O	*−3.18*	*5.96E-06*	*−2.42*	*1.68E-05*
Xylb//xylulokinase homolog (H. influenzae) –U	−3.19	1.70E-06	−2.51	4.54E-06
Lhfp//lipoma HMGIC fusion partner –U	−3.19	4.12E-06	−2.65	8.66E-06
Prkag2//protein kinase, AMP-activat gamma 2 (4) –O	**−3.20**	**3.79E-06**	**−2.61**	**8.39E-06**
Six2//SIX homeobox 2 (1) –T	−3.20	3.23E-06	−2.19	1.19E-05
Uri1//URI1, prefoldin-like chaperone –T	−3.21	4.03E-06	−3.34	5.07E-06
Aarsd1//alanyl-tRNA synthetase domain containing 1–T	−3.21	1.80E-05	−3.10	2.46E-05
Pik3r2//phosphoinositide-3-kinase, regulatory subunit 2- O	*−3.22*	*1.03E-05*	*−2.96*	*1.62E-05*
Mkrn2//makorin, ring finger protein, 2–O	−3.22	6.43E-05	−2.84	1.16E-04
Map9//microtubule-associated protein 9–D	−3.25	1.70E-05	−2.97	2.74E-05
Dnajc2//DnaJ (Hsp40) homolog, subfamily C, memb 2–T	−3.25	1.73E-05	−2.29	7.41E-05
Asb13//ankyrin repeat and SOCS box-containing 13–O	−3.26	3.47E-06	−2.65	7.73E-06

Table 2. Cont.

Gene symbol//gene title (ref #) – functional categories	K+-free medium		ouabain	
	Fold change	p value	Fold change	p value
RGD1561270//similar to zinc finger protein 248–T	−3.26	2.32E-05	−3.71	2.04E-05
Hebp2//heme-binding protein 2–O	−3.26	6.69E-05	−2.54	2.00E-04
Cers4//ceramide synthase 4–O	−3.28	5.44E-05	−2.94	9.07E-05
MGC108823//similar to interferon-inducible GTPase –U	−3.28	1.20E-04	−3.17	1.52E-04
Bmyc//brain expressed myelocytomatosis oncogene –T	*−3.28*	*2.90E-05*	*−3.01*	*4.61E-05*
Pitpna//phosphatidylinositol transfer protein, alpha –O	−3.28	9.08E-07	−2.84	2.91E-06
Npepl1//aminopeptidase-like 1 – O	−3.29	7.69E-06	−3.32	9.65E-06
Mtrr//5-methyltetrahydrofolate-homocystein (2) –O	**−3.29**	**1.07E-05**	**−3.02**	**1.73E-05**
Akap6//A kinase (PRKA) anchor protein 6–O	−3.30	3.74E-05	−3.60	3.49E-05
Ttc8//tetratricopeptide repeat domain 8–D	−3.30	5.05E-06	−3.72	5.61E-06
Dgcr8//DiGeorge syndrome critical region gene 8–T	−3.30	2.90E-06	−1.70	3.90E-05
Mgat4b//mannosyl (alpha-1,3-)-glycoprotein beta –O	−3.30	3.01E-05	−3.84	2.40E-05
LOC687284//similar to excision repair cross-complem –U	−3.32	2.05E-05	−3.60	2.05E-05
Rpusd1//RNA pseudouridylate synthase domain-cont –T	−3.32	1.85E-05	−2.74	4.20E-05
LOC500420//similar to CG12279-PA –U	−3.33	2.38E-04	−5.21	7.30E-05
Stxbp2//syntaxin-binding protein 2–O	−3.33	9.86E-06	−4.00	8.49E-06
Mis18bp1//MIS18-binding protein 1–U	−3.34	6.29E-06	−1.76	1.02E-04
Nol3//nucleolar protein 3, apoptosis repressor (16) – D	**−3.34**	**4.84E-05**	**−2.16**	**3.44E-04**
Lst8//MTOR-associated protein, LST8 homolog – T	−3.34	1.25E-05	−2.80	2.66E-05
Bbs9//Bardet-Biedl syndrome 9–O	−3.35	6.12E-06	−2.70	1.38E-05
Apip//APAF1-interacting protein (1) –D	**−3.35**	**9.85E-06**	**−3.22**	**1.35E-05**
Rabif//RAB-interacting factor (1) –O	**−3.35**	**9.08E-07**	**−1.71**	**7.26E-06**
Vsnl1//visinin-like 1–O	*−3.36*	*1.00E-04*	*−3.19*	*1.37E-04*
Fig4//FIG4 homolog, SAC1 lipid phosphatase domain –O	−3.37	9.33E-06	−3.14	1.37E-05
Tmem209//transmembrane protein 209–U	−3.37	1.96E-05	−4.16	1.46E-05
LOC685574//zinc finger protein 334-T	−3.38	3.36E-05	−3.18	4.91E-05
Arhgef25//Rho guanine nucleotide exchange factor 25–D	−3.40	5.05E-06	−3.13	8.33E-06
Vamp4//vesicle-associated membrane protein 4–O	−3.40	1.52E-04	−2.58	5.08E-04
Pold2//polymerase (DNA directed), delta 2, regulat sub –D	−3.40	2.88E-05	−2.06	2.70E-04
Ssbp1//single-stranded DNA-binding protein 1–O	−3.40	6.62E-06	−3.45	8.57E-06
Slc35d2//solute carrier family 35, member D2–O	−3.40	6.67E-06	−3.32	9.24E-06
LOC683626//similar to limb-bud and heart –U	−3.41	1.30E-05	−1.84	2.13E-04
Lrrk1//leucine-rich repeat kinase 1–O	−3.41	4.33E-05	−3.31	5.60E-05
RGD1309362//similar to interferon-inducible GTPase –O	−3.41	1.21E-04	−3.64	1.10E-04
Acat3//acetyl-coenzyme A acetyltransferase 3–O	−3.41	4.09E-06	−2.35	1.42E-05
Pter//phosphotriesterase related –O	−3.42	8.74E-06	−2.31	3.69E-05
RragB//Ras-related GTP-binding B–D	−3.43	1.93E-04	−2.56	7.02E-04
Pdcd4//programmed cell death 4 (5) –D	**−3.43**	**1.28E-05**	**−1.74**	**3.18E-04**
Aaas//achalasia, adrenocortical insufficiency, alacrimia – O	−3.44	3.64E-06	−2.53	1.03E-05
Bphl//biphenyl hydrolase-like (serine hydrolase) O	−3.45	1.38E-05	−3.96	1.28E-05
Zfp68//zinc finger protein 68–T	−3.45	1.17E-03	−3.40	1.31E-03
Stambp//Stam-binding protein –I	−3.45	2.04E-05	−4.59	1.33E-05
Ptcd2//pentatricopeptide repeat domain 2–U	−3.46	2.03E-04	−4.01	1.41E-04
Aurkb//aurora kinase B–D	−3.47	8.48E-06	−1.84	1.24E-04
Mvd//mevalonate (diphospho) decarboxylase –O	−3.49	5.26E-05	−2.07	5.61E-04
Ssh3//slingshot homolog 3 (Drosophila) –O	−3.50	1.82E-06	−3.39	3.26E-06
Zfp110//zinc finger protein 110–T	−3.50	1.03E-05	−3.33	1.46E-05
Hscb//HscB iron-sulfur cluster co-chaperone homolog – O	*−3.50*	*2.66E-05*	*−3.00*	*5.16E-05*

Table 2. Cont.

Gene symbol//gene title (ref #) – functional categories	K⁺-free medium		ouabain	
	Fold change	p value	Fold change	p value
Tfip11//tuftelin-interacting protein 11–D	−3.51	5.98E-06	−4.67	5.00E-06
Thtpa//thiamine triphosphatase/-O	−3.52	1.26E-05	−3.27	1.96E-05
LOC100362431//tetratricopeptide repeat domain 30B –U	−3.52	2.88E-05	−3.00	5.70E-05
RGD1564300//similar to phosphoseryl-tRNA kinase –U	−3.53	2.95E-05	−3.91	2.74E-05
Lrrc8e//leucine-rich repeat containing 8 family, memb E – D	−3.53	3.20E-04	−4.51	1.63E-04
Zfp39//zinc finger protein 39–T	−3.54	1.22E-04	−3.72	1.18E-04
Fbxl4//F-box and leucine-rich repeat protein 4–D	−3.55	1.87E-06	−3.72	3.17E-06
Mpped2//metallophosphoesterase domain containing 2 – O	−3.55	2.65E-05	−3.28	4.02E-05
Trak2//trafficking protein, kinesin binding 2–O	−3.55	8.54E-06	−2.34	3.83E-05
Ecsit//ECSIT homolog (Drosophila) –O	−3.55	1.18E-05	−3.75	1.34E-05
Tdp1//tyrosyl-DNA phosphodiesterase 1–D	−3.55	9.58E-06	−4.83	7.04E-06
Pik3c2b//phosphoinositide-3-kinase, class 2, beta-O	−3.56	1.12E-05	−3.20	1.86E-05
Nexn//nexilin (F actin binding protein) –D	−3.59	8.85E-05	−2.98	1.92E-04
Impa2//inositol (myo)-1(or 4)-monophosphat 2 (1) - O	**−3.60**	**7.30E-05**	−2.24	**5.86E-04**
Oasl2//2′-5′ oligoadenylate synthetase-like 2-T	−3.60	4.54E-05	−4.51	3.03E-05
Stk25//serine/threonine kinase 25 (1) –O	**−3.60**	**3.32E-06**	−2.97	**6.95E-06**
Cnpy2//canopy 2 homolog (zebrafish) –D	−3.61	1.13E-05	−3.23	1.91E-05
Mrvi1//murine retrovirus integration site 1 homolog – U	−3.62	3.34E-06	−4.17	4.06E-06
Mrpl40//mitochondrial ribosomal protein L40 –T	−3.62	2.39E-05	−3.43	3.39E-05
Plin3//perilipin 3//9q11//316130 –O	−3.63	8.44E-06	−2.34	4.00E-05
Fam118a//family with sequence similarity 118, mem A –U	−3.64	5.05E-06	−4.01	6.02E-06
Mmd//monocyte to macrophage differentiation-ass – U	−3.65	1.43E-05	−2.83	3.77E-05
Hddc2//HD domain-containing 2 – U	−3.66	1.49E-05	−3.68	1.88E-05
Zfp386//zinc finger protein 386 (Kruppel-like) – T	−3.67	1.00E-04	−3.02	2.20E-04
Ficd//FIC domain-containing –O	−3.67	7.72E-06	−3.04	1.56E-05
Wdr11//WD repeat domain 11–T	−3.68	2.74E-05	−5.73	1.32E-05
Xrcc6//X-ray repair complement defective repair – D	−3.68	1.18E-05	−2.37	6.06E-05
Stx17//syntaxin 17–D	−3.68	1.03E-05	−5.02	7.40E-06
LOC100362548//rCG52086-like – U	−3.70	4.60E-06	−2.04	3.71E-05
Nipsnap3b//nipsnap homolog 3B (C. elegans) –O	−3.71	1.64E-05	−1.95	2.63E-04
Cad//carbamoyl-phosphate synthetase 2 –O	−3.72	1.09E-05	−2.72	3.33E-05
Gemin4//gem (nuclear organelle) associated protein 4 – T	−3.73	3.95E-05	−4.65	2.74E-05
Nagk//N-acetylglucosamine kinase –O	−3.73	4.98E-06	−4.28	5.47E-06
Tamm41//TAM41, mitochondrial translocator assembly – O	−3.73	7.27E-06	−2.99	1.61E-05
Msto1//misato homolog 1 (Drosophila) –O	−3.74	1.23E-05	−3.57	1.77E-05
Mutyh//mutY homolog (E. coli) (3) –D	**−3.76**	**9.85E-06**	−3.14	**1.91E-05**
Stat2//signal transducer, activator of transcrip 2 (3) – T	**−3.76**	**1.50E-06**	−4.33	**2.78E-06**
Gcs1//glucosidase 1–O	−3.81	3.65E-05	−2.03	5.66E-04
Ccdc36//coiled-coil domain containing 36–U	−3.84	2.43E-06	−2.85	6.65E-06
Odf3l1//outer dense fiber of sperm tails 3-like 1–U	−3.88	1.54E-05	−4.58	1.37E-05
LOC100360582//5′,3′-nucleotidase, cytosolic –O	−3.89	3.03E-05	−2.48	1.69E-04
Dguok//deoxyguanosine kinase –O	−3.90	2.09E-05	−3.00	5.56E-05
Ick//intestinal cell kinase –D	−3.90	7.69E-06	−3.30	1.43E-05
Aspscr1//alveolar soft part sarcoma chrom region 1 – O	−3.92	4.86E-06	−2.01	5.15E-05
Arntl2//aryl hydrocarbon receptor nuclear transl-like 2 – T	−3.93	3.45E-06	−2.92	8.57E-06
Acy3//aspartoacylase (aminocyclase) 3–O	−3.93	3.79E-06	−3.47	6.91E-06
Zfp9//zinc finger protein 9–T	−3.99	6.67E-06	−3.71	1.02E-05
LOC688548//hypothetical protein LOC688548–U	−3.99	3.08E-05	−3.06	8.11E-05

Table 2. Cont.

Gene symbol//gene title (ref #) – functional categories	K$^+$-free medium		ouabain	
	Fold change	p value	Fold change	p value
Fblim1//filamin-binding LIM protein 1–D	−4.01	5.05E-06	−3.87	7.42E-06
Kif3c//kinesin family member 3C –O	−4.01	1.69E-05	−3.32	3.48E-05
Gsdmd//gasdermin D –D	−4.02	3.08E-06	−3.36	6.02E-06
LOC498145//similar to RIKEN cDNA 2810453I06 –U	−4.02	2.45E-04	−2.89	8.91E-04
Zfp426l2//zinc finger protein 426-like 2–T	−4.02	5.00E-05	−4.59	4.24E-05
Chst12//carbohydrate (chondroitin 4) sulfotransfer 12– O	−4.03	1.13E-05	−2.89	3.48E-05
RGD1565316//similar to sphingomyelin phosphodies – U	−4.04	7.16E-06	−4.18	8.72E-06
Mir143//microRNA mir-143 – T	−4.04	4.55E-05	−2.67	2.14E-04
Sh3glb2//SH3-domain GRB2-like endophilin B2 – U	−4.04	4.68E-05	−2.05	8.75E-04
Ccdc8//coiled-coil domain-containing 8 – D	−4.06	1.20E-05	−2.98	3.48E-05
Pot1//protection of telomeres 1 homolog (1) – D	**−4.07**	**5.28E-06**	**−5.21**	**5.01E-06**
Rbl2//retinoblastoma-like 2 – T	−4.07	5.76E-06	−2.05	6.46E-05
Ankra2//ankyrin repeat, family A (RFXANK-like) 2 – O	−4.09	1.26E-05	−4.30	1.44E-05
Slc45a4//solute carrier family 45, member 4 – O	−4.10	5.05E-06	−2.92	1.45E-05
Polm//polymerase (DNA directed) – D	−4.13	4.22E-06	−4.06	6.03E-06
Hmbs//hydroxymethylbilane synthase (1) – O	**−4.16**	**3.51E-06**	**−2.76**	**1.15E-05**
Mrpl40//mitochondrial ribosomal protein L40 – T	−4.17	1.45E-04	−4.20	1.59E-04
Fastk//Fas-activated serine/threonine kinase – T	−4.20	9.96E-06	−2.84	3.50E-05
LOC688548//hypothetical protein LOC688548 – U	−4.29	1.31E-05	−3.27	3.31E-05
LOC691254//hypothetical protein LOC691254 – U	−4.39	1.05E-05	−4.31	1.37E-05
Plcb3//phospholipase C, beta 3, PIP-specific (1) – O	**−4.41**	**2.75E-06**	**−3.20**	**7.06E-06**
Setd6//SET domain-containing 6 – T	−4.41	5.99E-06	−3.55	1.22E-05
RGD1565222//similar to RIKEN cDNA 4931414P19 – U	−4.43	1.17E-05	−3.74	2.18E-05
Crot//carnitine O-octanoyltransferase – O	−4.44	1.26E-05	−3.59	2.66E-05
Haus1//HAUS augmin-like complex, subunit 1 – D	−4.46	3.39E-05	−4.58	3.85E-05
Paqr7//progestin and adipoQ receptor family memb VII – O	−4.52	3.81E-06	−5.24	4.54E-06
Slc27a4//solute carrier family 27 (fatty acid transp) – O	−4.56	1.11E-05	−3.03	3.94E-05
Pde6d//phosphodiesterase 6D, cGMP-specific, rod – O	−4.57	5.23E-06	−5.82	5.06E-06
Stard3nl//STARD3 N-terminal like – O	−4.61	2.60E-06	−3.88	5.04E-06
Ssx2ip//synovial sarcoma, X breakpoint 2 interact prot – D	−4.64	1.05E-05	−3.20	3.31E-05
Galk1//galactokinase 1 – O	−4.68	1.03E-05	−4.08	1.73E-05
Nipsnap1//nipsnap homolog 1 (C. elegans) – O	−4.72	9.38E-06	−4.94	1.08E-05
Golph3l//golgi phosphoprotein 3-like – O	−4.75	2.90E-06	−3.34	7.44E-06
Kprp//keratinocyte proline-rich protein – U	−4.79	5.45E-05	−5.63	4.47E-05
Nr1h2//nuclear receptor subfamily 1, group H, mem 2 – T	−4.94	3.81E-05	−4.03	7.47E-05
Ogg1//8-oxoguanine DNA glycosylase (11) – D	**−5.11**	**4.60E-06**	**−3.10**	**1.68E-05**
Nsdhl//NAD(P)-dependent steroid dehydrogenase-like – O	−5.13	9.08E-07	−3.59	2.89E-06
Mir145//microRNA mir-145 – T	−5.14	1.50E-06	−3.36	4.54E-06
Zfp40//zinc finger protein 40 – T	−5.20	7.56E-06	−4.07	1.54E-05
RGD1311946//similar to RIKEN cDNA 1810055G02 – U	−5.28	1.87E-06	−6.39	2.95E-06
Tmem177//transmembrane protein 177 – O	−5.41	3.53E-05	−7.49	2.30E-05
Rab27a//RAB27A, member RAS oncogene family – T	−5.65	3.45E-06	−6.40	4.47E-06
Stx2//syntaxin 2 – D	−5.82	2.27E-06	−4.98	4.54E-06
Stk16//serine/threonine kinase 16 – O	−6.35	1.70E-06	−5.32	3.58E-06
Ttc30b//tetratricopeptide repeat domain 30B – O	−7.12	8.89E-06	−7.00	1.13E-05

Table 2. Cont.

Gene symbol//gene title (ref #) – functional categories	K$^+$-free medium		ouabain	
	Fold change	p value	Fold change	p value
Tradd//TNFRSF1A-associated via death domain (5) – T	**−7.81**	**9.08E-07**	**−7.44**	**1.84E-06**
Zinki//Arg3.1/Arc mRNA-binding zinc finger protein – T	−8.80	3.51E-06	−7.78	5.65E-06

RVSMC were treated with 3 mM ouabain or K$^+$-free medium for 6 hr. Listed are assigned genes whose expression was decreased in K$^+$-free medium by more than 3-fold and was different by less than 2-fold in the presence of ouabain compared to K$^+$-free medium. GeneChip expression analysis was performed as described in the Methods section. mRNA content in control cells was taken as 1.00. Genes whose expression is altered in ischemia/hypoxia are shown **in bold**. Appearing in parentheses are numbers of citations in PubMed. Given *in italics* are genes whose differential expression was detected in ischemic tissue by whole genome microarray-based analysis [12–18]. Data on gene function from GeneCards database (www.genecards.org) were used for identification of gene function. Functional categories: T– regulators of transcription/translation, RNA processing and degradation; D– regulators of cell adhesion, migration, proliferation, differentiation and death; I– inflammation and immune responses; O – others; U – unknown function.
doi:10.1371/journal.pone.0110597.t002

Second, 24-hr maintenance of RASMC under hypoxic, glucose-depleted conditions resulted in ~3-fold elevation of $[Na^+]_i$ and 2-fold attenuation of $[K^+]_i$ (Fig. 2). Previously, it was shown that transient ischemia of cardiac myocytes increased $[Na^+]_i$ from 5-8 to 25–40 mM and decreased $[K^+]_i$ by 30% [48]. Augmentation of

the $[Na^+]_i/[K^+]_i$ ratio observed in hypoxic RASMC is probably caused by attenuation of intracellular ATP content (Fig. 2) that, in turn, leads to partial inhibition of Na$^+$,K$^+$-ATPase.

Third, RASMC transfection with *Hif-1a* siRNA curbed the increment of HIF-1α protein as well as *Vegfa, Edn1, Klf10* and

Table 3. Hypoxia-responsive transcription factors whose expression was increased in RASMC subjected to Na$^+$,K$^+$-ATPase inhibition.

Gene symbol Gene title		Fold alterations	
		K$^+$-free	ouabain
HIF			
Hif-1b/Arnt	Aryl hydrocarbon receptor nuclear translocator	1.28	1.24
Ahr	Aryl hydrocarbon receptor	1.94	1.34
NFkB			
Ikbkg	Inhibitor of kappa light polypeptide kinase β	−1.93	−3.06
Ikbke	Inhibitor of kappa light polypeptide kinase ε	−2.16	−2.18
Sike 1	Suppressor of Ikbke	−5.51	−6.40
AP-1			
Fos	FBJ osteosarcoma oncogene	7.91	3.95
Jun	Jun proto-oncogene	3.57	2.76
Junb	Jun B proto-oncogene	3.23	1.29
Jund	Jun D proto-oncogene	1.59	1.53
Atf3	Activating transcription factor 3	7.83	4.53
Atf6	Activating transcription factor 6	1.42	1.36
Atf1	Activating transcription factor 1	1.35	1.24
Maff	v-maf musculoaponeurotic oncogene homolog F	3.42	2.55
Mafk	v-maf musculoaponeurotic oncogene homolog K	3.42	2.75
CREB			
Creb5	cAMP-responsive element-binding protein 5	1.69	1.36
Creb1	cAMP-responsive element-binding protein 1	1.45	1.46
p53			
Mdm2	Mdm2 p53-binding protein homolog (mouse)	3.85	2.98
EGR			
Egr1	Early growth response 1	5.15	1.49
OTHERS			
Sp1	Sp1 transcription factor	2.00	1.50

Na$^+$,K$^+$-ATPase was inhibited for 6 hr by 3 mM ouabain or K$^+$-free medium. Expression of other genes encoding members of HIF-1 (*Hif-1a, Hif-2a, Hif-3a*), NFκB (*p65, cRel, RelB, p50, p52, IκB*) as well as other hypoxia-inducible transcription factors (*p53, Sp3, Gata2, Stat5, Gadd153*) was not significantly changed.
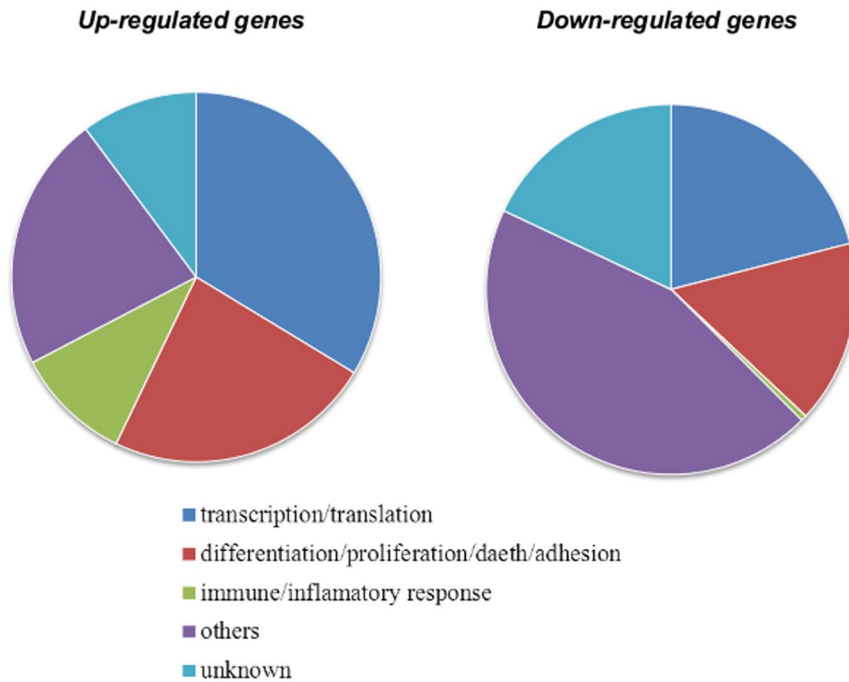doi:10.1371/journal.pone.0110597.t003

Figure 5. Distribution of up- and down- regulated [Na$^+$]$_i$/[K$^+$]$_i$-sensitive genes listed in Tables 2 and 3 among major functional categories.
doi:10.1371/journal.pone.0110597.g005

Nr4a1 mRNA triggered by ischemia (but did not significantly affect the ~7-, 5-, 4- and 3-fold elevation of *Atf3, Ptgs2, Fos* and *Per2* expression documented in hypoxic cells (Figs. 6 and 7, Table 4).

Fourth, unlike *Hif-1a* siRNA, dissipation of the transmembrane gradients of monovalent cations in low-Na$^+$, high-K$^+$ medium abolished the increase of *Fos, Atf3, Ptgs2* and *Per2* mRNA and sharply decreased *Klf10, Edn1, Nr4a1* and *Hes1* expression evoked by hypoxia. Significantly, low-Na$^+$, high-K$^+$ medium completely abrogated elevation of the [Na$^+$]$_i$/[K$^+$]$_i$ ratio (Fig. 2) as well as increments of the expression of all investigated genes seen in ouabain-treated RASMC (Table 4, Fig. 7).

Viewed collectively our results demonstrate the dominated role of [Na$^+$]$_i$/[K$^+$]$_i$-mediated excitation-transcription coupling in overall transcriptomic changes triggered by ischemic conditions. It was shown that in ischemic tissues HIF-1α increases expression of *Vegfa* and *Edn1* via interaction of HIF-1α/HIF-1β heterodimer with hypoxia response elements (HRE) encoding by 5′-UTR (A/G)CGTG consensus [45;46;49]. We noted that side-by-side with *Hif-1a* siRNA-sensitive *Vegfa* and *Edn1*, 5′-UTRs of *Hif-1a* siRNA-resistant *Atf3, Ptgs2, Fos* and *Per2* are also abundant with (A/G)CGTG sequences (Fig. 8 and 9). Therefore, the presence of (A/G)CGTG consensus within 5′-UTR is not sufficient alone to predict HIF-1-mediated mechanism of gene expression regulation in hypoxic conditions.

Side-by-side with HIF-1α protein accumulation, hypoxia triggers the expression of other transcription factors listed in Table 3 and reviewed by Cummins et al. [33]). Do these transcription factors contribute to [Na$^+$]$_i$/[K$^+$]$_i$-mediated transcriptomic changes evoked by hypoxia? We found a negligible impact of Na$^+$,K$^+$-ATPase inhibition on *Hif-1β* expression and 2-fold elevation of mRNA encoding aryl hydrocarbon receptors for dioxins, benzopyrenes and other environmental pollutions (AhR) (Table 3). It was shown that, in addition to HIF-1α, HIF-1β forms a dimer with AhR [50] that leads to similar expression levels of the

P450 isoforms CYP1A1 and CYP1B1 via binding of AhR/HIF-1β complex to the TNGCGTG consensus sequence in xenobiotic-responsive elements [44;51]. However, the involvement of this regulatory pathway in the expression of [Na$^+$]$_i$/[K$^+$]$_i$-sensitive genes seems unlikely. Indeed, we observed very modest elevation of *Cyp1b1* expression elicited by ouabain and K$^+$-free medium (1.41- and 1.54-fold, respectively), in contrast to the ~15-fold increase of *Cyp1a1* expression (Table 1). We did not find any changes in mRNAs encoding regulatory (*p65, cRel, RelB, p50, p52*) and inhibitory (*IκB*) subunits of NFκB. *Ikbkg* and *Ikbke* encode kinases that phosphorylate IkB, causing its dissociation and activation of NFkB-mediated transcription, whereas SIKE1 interacts with *Ikbke* and inhibits it [52]. Both *Ikbkg/Ikbke* and *Sike1* expression was decreased up to 5-fold by ouabain and K$^+$-free medium (Table 3). Thus, the final outcome of elevation of the [Na$^+$]$_i$/[K$^+$]$_i$ ratio on the activity of this regulatory pathway remains unknown. MDM2 is a major negative regulator of p53. Elevation of the [Na$^+$]$_i$/[K$^+$]$_i$ ratio increased *Mdm2* expression by ~3-fold (Table 3), suggesting inhibition of p53 transcription rather than activation detected in hypoxia [53]. We observed that 6-hr inhibition of the Na$^+$,K$^+$-ATPase resulted in 2–3-fold attenuation of mRNAs encoding AMP-activated protein kinase (AMPK) regulatory subunits *Prkag1* and *Prag2* (Table 2). These data suggest that elevation of the [Na$^+$]$_i$/[K$^+$]$_i$ ratio attenuates rather than activates AMPK whose augmented activity was detected in hypoxic cells [53;54].

Previously, we demonstrated that 3-hr inhibition of Na$^+$,K$^+$-ATPase in RASMC by ouabain and K$^+$-free medium augmented *Egr1* by ~5 and 7-fold, respectively [26]. Prolongation of incubation time up to 6 hr decreased the increments of *Egr1* mRNA (Table 3), suggesting transient activation of this transcription factor. We also documented activation of the transcription factor AP-1, indicated by up to 8-fold augmentation of mRNAs encoding its major subunits, including *Fos, Jun, Atf3, Maff* and *Mafk* (Table 3). These data show that AP-1 and Egr1 are major

Table 4. Effect of high-K$^+$, low-Na$^+$ medium and *Hif-1α* siRNA on gene expression triggered by hypoxia and ouabain.

Gene symbol	Cell treatment											
	Control (High-Na$^+$, low-K$^+$)			Low-Na$^+$, high-K$^+$			Scrambled siRNA			HIF-1α siRNA		
	normoxia	hypoxia	ouabain	normoxia	hypoxia	ouabain	normoxia	hypoxia	ouabain	normoxia	hypoxia	ouabain
Hif-1a	1.00	1.88±11	1.56±18	0.8±8	1.25±5	1.06±21	0.89±14	1.47±13	1.11±9	0.31±4	0.26±4	0.22±5
Vegfa	1.00	12.67±248	1.43±16	1.42±7	14.53±168	1.11±18	0.77±13	11.19±98	1.08±6	0.89±21	3.12±5	1.36±23
Edn1	1.00	4.11±39	2.45±11	1.07±8	2.85±26	0.87±16	1.14±22	4.89±54	2.66±17	1.14±9	1.89±44	2.46±2
Cypa1	1.00	0.43±4	8.94±111	1.33±22	0.39±7	1.76±25	0.95±15	0.38±6	10.25±211	0.77±21	0.40±4	13.17±311
Fos	1.00	4.12±41	5.21±16	1.99±29	2.02±17	1.65±28	0.87±17	5.11±48	5.07±12	1.12±18	4.01±38	4.77±29
Atf3	1.00	7.16±53	5.02±65	2.19±3	3.13±4	2.02±17	1.07±28	6.92±58	5.00±82	0.98±9	3.12±3	5.14±37
Klf10	1.00	5.02±66	4.06±44	1.19±1	2.18±4	1.33±31	1.07±9	3.87±36	4.56±42	1.26±18	3.03±51	3.82±34
Ptgs2	1.00	5.14±77	9.87±138	2.12±42	1.88±19	1.98±31	1.23±7	6.11±1	9.67±132	0.92±13	4.91±57	9.16±49
Nr4a1	1.00	6.11±79	6.15±71	1.36±12	2.60±39	1.71±44	0.91±6	3.15±21	7.11±155	0.92±19	2.91±46	7.06±79
Per2	1.00	3.02±36	6.18±14	0.98±18	1.48±2	1.38±17	1.27±19	3.37±28	5.82±7	1.06±19	3.00±32	7.59±131
Hes1	1.00	1.72±46	3.48±33	1.56±18	2.09±28	1.89±22	0.87±9	1.30±27	3.22±43	1.16±23	1.03±15	4.09±58

Control non-transfected RASMC or RASMC transfected with scrambled or *Hif-1α* siRNA were exposed to hypoxia/glucose deprivation or 3 mM ouabain in control or low-Na$^+$, high-K$^+$ medium for 24 hr and RNAs content of genes listed in the left column was quantified by real-time quantitative RT-PCR as described in Methods. Means ± S.E. obtained in 3 independent experiments performed in triplicate are shown. Mean values for cells incubated in control medium under normoxic conditions were taken as 1.00.
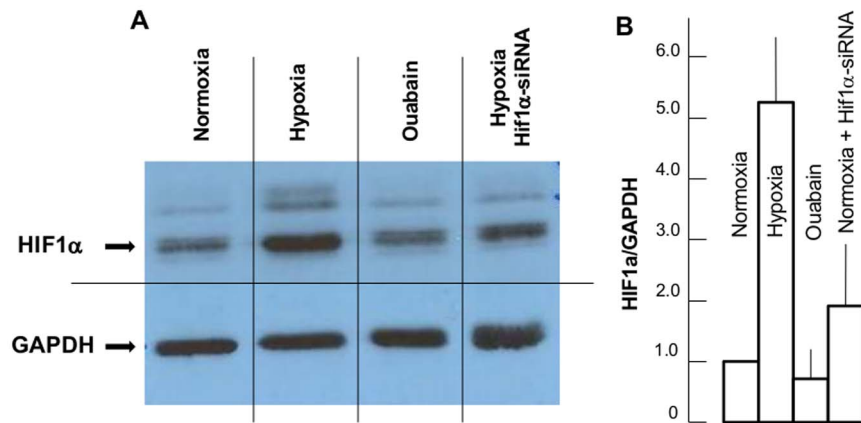doi:10.1371/journal.pone.0110597.t004

Figure 6. A. Representative Western blots of HIF-1α and GAPDH in RASMC subjected to 24-hr incubation under control conditions (normoxia), hypoxia/glucose deprivation, 3 mM ouabain or hypoxia/glucose deprivation in cells transfected with *Hif-1α* siRNA. **B**. Effect of hypoxia/glucose deprivation and ouabain on relative content of HIF-1α protein in RASMC. The HIF-1α/GAPDH ratio in control conditions was taken as 1.00. Data obtained in 3 independent experiments are reported as means ± S.E.
doi:10.1371/journal.pone.0110597.g006

hypoxia-inducible transcriptions factors that are also activated by elevation of the $[Na^+]_i/[K^+]_i$ ratio. Yan and co-workers reported that hypoxia triggered Egr1 in cultured hepatoma-derived cells deficient in HIF-1β [55]. We state here that Fos mRNA accumulation triggered by ouabain occurs in HIF-1α-deficient RASMC (Table 4), indicating that that both the Egr1 and AP-1 pathways are initiated in response to oxygen deprivation independently of HIF-1. As an alternative hypothesis, we propose that activation of *Egr1*, AP-1 and other *Hif-1α* siRNA-resistant genes listed in Table 4 in hypoxic cells is mediated by ATP depletion, Na+,K+-ATPase inhibition and dissipation of the transmembrane gradients of monovalent cations (Fig. 10).

It was shown that gain of Na^+_i rather than loss of K^+_i sparks augmented Fos expression in RASMC [56]. Numerous studies have disclosed that $[Na^+]_i$ elevation heightens $[Ca^{2+}]_i$ via activation of Na^+_i/Ca^{2+}_o exchanger as well as via depolarization and activation of voltage-gated Ca^{2+} channels (for review, see [57;58]). It has been well-documented that $[Ca^{2+}]_i$ elevation affects gene expression by activation of cAMP-response elements via CREB phosphorylation by (Ca^{2+}+calmodulin)-dependent protein kinase and nuclear factor AT (NFAT) dephosphorylation by

calcineurin [59]. In previous investigation, we found that addition of extracellular (EGTA and intracellular (BAPTA) Ca2+ chelators increased rather than decreased the number of $[Na^+]i/[K^+]i$-sensitive genes [26]. It should be noted, however, that these compounds may affects cellular functions independently of Ca^{2+} depletion. Thus, we observed that addition of EGTA increases permeability of vascular smooth muscle cells for Na^+ [60]. Thus, additional experiments should be performed to clarify relative impact of Ca^{2+}-mediated and -independent signaling shown in Fig. 10 in transcriptomics changes evoked by hypoxia.

Conclusion

We report here that elevation of the $[Na^+]_i/[K^+]_i$ ratio contributes to transcriptomic changes triggered by hypoxia and glucose deprivation independently of HIF-1—mediated signalling. The molecular origin of the upstream sensor and the relative contribution of the gain of $[Na^+]_i$ and loss of $[K^+]_i$ in the triggering of this novel signalling pathway, including the augmented expression of hypoxia-inducible Egr1 and AP-1 transcription factors, remains unknown. Recent studies have demonstrated that modulation of histone methylation via an epigenetic mechanism is

Table 5. Primer sequences for RT-PCR.

| Gene symbol	Forward primers	Reverse primers
Atf3	TGTCAGTCACCAAGTCTGAGGT	CAGTTTCTCTGACTCCTTCTGC
Cyp1a1	ATTTGAGAAGGGCCACATCC	AAACCCAGCTCCAAAGAGGT
Edn1	AAAGAACTCCGAGCCCAAAG	CTGATGGCCTCCAACCTTC
Fos	GAGCAGCTATCTCCTGAAGAGG	TGATCTGTCTCCGCTTGGA
Hes1	CAAACCAAAGACAGCCTCTGA	ATGCCGGGAGCTATCTTTCT
Hif1a	AAAGCTCACCTGAGCCTAACA	TGTCCTGAGCTGAAAATGGA
Klf10	TCTGTAGCCACCCAGGATGT	GGACAGTTCATCGGAACGAG
Nr4a1	GATGCCTCCCCTACCAATCT	GTCACCGGCATCTTCCTTT
Per2	GCAGGTGAAGGCTAATGAGG	CACAGCAAACATGTCCGAGT
Ptgs2	GGCCATGGAGTGGACTTAAA	TGTCTTTGACTGTGGGAGGA
Vegfa2	CATGCGGATCAAACCTCAC	TGGCTTTGTTCTATCTTTCTTTGG

doi:10.1371/journal.pone.0110597.t005
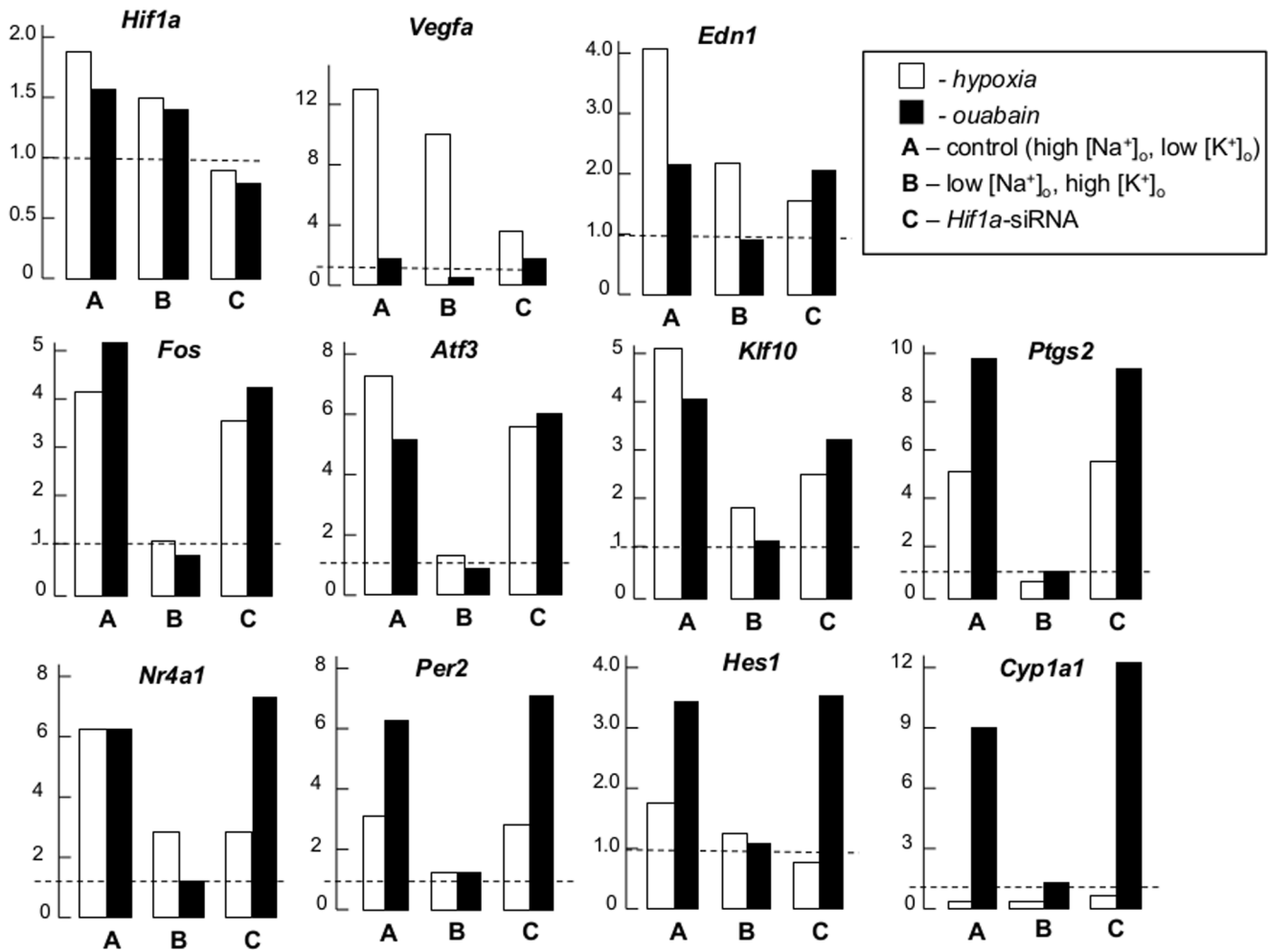
Figure 7. Effect of hypoxia and ouabain on gene expression in RASMC. Cells were exposed to normoxia, hypoxia/glucose deprivation or 3 mM ouabain for 24 hr in control high-Na+, low-K+ medium (**A, C**), or high-K+, low-Na+ medium (**B**). In some experiments, RASMC were transfected with *Hif-1α* siRNA (**C**). mRNA content in normoxia was taken as 1.00 and shown by broken lines. For more details, see figure 4 legend.
doi:10.1371/journal.pone.0110597.g007

a key device that cells use to adapt to hypoxia [61]. Increasing evidence indicates that side-by-side with regulation of the 5′-UTR by transcription factors, gene activation or silencing is under the

complex control of 3-dimensional positioning of genetic materials and chromatin in nuclear spaces [62;63]. The role of the $[Na^+]_i/[K^+]_i$ ratio in the epigenetic regulation of 3-dimensional genome
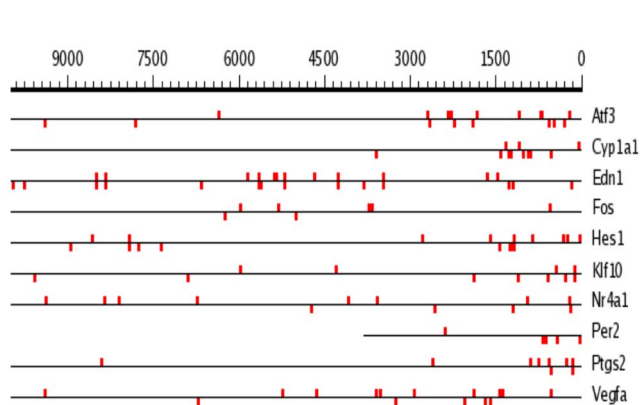
Figure 8. Position of (A/G)CGTG consensus within 10,000 bp 5′-UTR of genes listed in Table 5.
doi:10.1371/journal.pone.0110597.g008
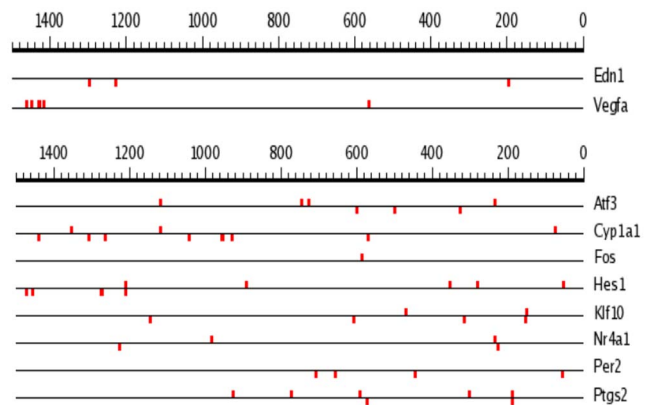
Figure 9. Position of (A/G)CGTG consensus within 1,500 bp 5′-UTR of genes listed in Table 5.
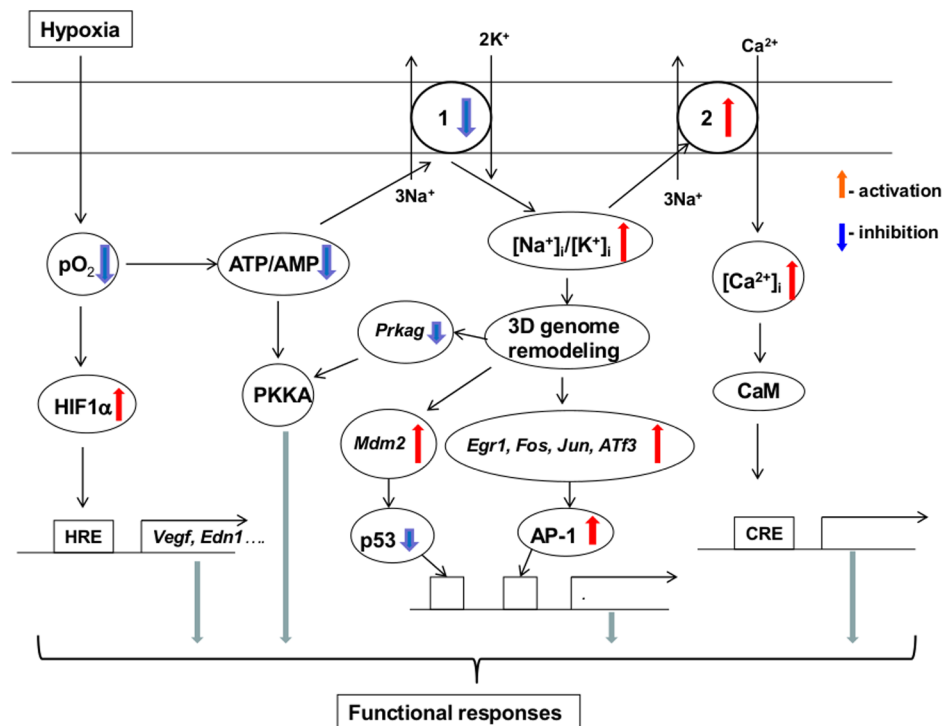doi:10.1371/journal.pone.0110597.g009

Figure 10. Possible mechanisms of the involvement of elevated $[Na^+]_i/[K^+]_i$ ratio in the transcriptomic changes evoked by hypoxia: a working hypothesis. 1– Na^+,K^+-ATPase; 2– Na^+/Ca^{2+} exchanger; CaM – calmodulin; CRE – Ca^{2+}-response elements. For other abbreviations, see text.
doi:10.1371/journal.pone.0110597.g010

organization and its relationship to gene silencing and activation are currently being examined in our laboratory.

Methods

Cell culture

Rat aortic smooth muscle cells (RASMC), purchased from Lonza (Walkersville, MD, USA), were grown at $37°C$ in a CO_2 incubator in Dulbecco's modified Eagle medium (DMEM, Invitrogen, Carlsbad, CA, USA) supplemented with 10% fetal bovine serum (FBS), 100 U/ml penicillin, 100 µg/ml streptomycin, and subjected to less than 10 passages. To establish quiescence, the cells were incubated for 24 hr in media in which FBS concentration was reduced to 0.2%.

Cell treatment

Quiescent cells were washed with K^+-free DMEM (Sp-DMEM; Invitrogen) and incubated for 6 hr at $37°C$ in a humidified atmosphere with 5% CO_2/balance air in control DMEM, K^+-free DMEM and DMEM containing 3 mM ouabain. In some experiments, we used DMEM-like medium containing (in mM) NaCl 109.4; KCl 5.4; $CaCl_2$ 1.8; $MgSO_4$ 0.8; $NaHCO_3$ 29.8; NaH_2PO_4 0.9; HEPES 8.4; glucose 5, vitamins and amino acids at concentrations indicated for DMEM recipes ($[Na^+]_o = 140.1$ mM; $[K^+]_o = 5.4$) or low-Na^+, high-K^+ medium where NaCl was substituted by KCl ($[Na^+]_o = 30.7$ mM; $[K^+]_o = 114.8$). Previously, we reported that $[K^+]_o$ elevation caused RASMC depolarization that, in turn, increased Fos expression via activation of L-type voltage-gated Ca^{2+} channels [56]. To inhibit this signalling pathway, 0.1 µM nicardipine was added in certain experiments. To trigger hypoxia, RASMC were incubated in custom-designed, air-tight, flow-through cuvettes in media containing 0.5 mM

glucose under substitution of 5% CO_2/air by 5% CO_2/N_2. Eight hr after incubation in a CO_2/N_2 environment, pO2 was ∼30 mm Hg compared to ∼150 mmHg in normoxia. We did not observe any impact of these treatment protocols on RASMC survival, estimated by lactate dehydrogenase release, caspase-3 activity and chromatin cleavage (data not included).

Intracellular content of monovalent ions

Intracellular K^+, Na^+ and Cl^- content was measured as the steady-state distribution of extra- and intracellular ^{86}Rb, ^{22}Na and ^{36}Cl, respectively. To establish isotope equilibrium, cells growing in 12-well plates were preincubated for 3 hr in control or K^+-free medium (Sp-DMEM+Ca) containing 0.5 µCi/ml $^{86}RbCl$, 4 µCi/ml $^{22}NaCl$ or 3 $H^{36}Cl$ with ouabain added for the next 3 hr. To test the action of K^+-free medium, the cells were washed twice with ice-cold Sp-DMEM+Ca. Then, cells loaded with ^{22}Na or ^{36}Cl were transferred to Sp-DMEM+Ca containing $^{22}NaCl$ and $H^{36}Cl$, respectively, whereas cells loaded with ^{86}Rb were transferred to isotope-free Sp-DMEM+Ca. After 3 hr, they were transferred onto ice, washed 4 times with 2 ml of ice-cold medium W containing 100 mM $MgCl_2$ and 10 mM HEPES-tris buffer (pH 7.4). The washing medium was aspirated and the cells lysed with 1% SDS and 4 mM EDTA solution. Radioactivity of the incubation media and cell lysates was quantified, and intracellular cation content was calculated as A/am, where A was the radioactivity of the samples (cpm), a was the specific radioactivity of ^{86}Rb (K^+), ^{22}Na or ^{36}Cl in medium (cpm/nmol), and m was protein content (mg). For more details, see [64].

Intracellular ATP content

Intracellular ATP content was measured by assaying luciferase-dependent luminescence with ATP bioluminescent assay kit

(Sigma, St. Louis, MO, USA), as described in detail elsewhere [65].

Intracellula Na$^+$, K$^+$, Cl$^-$ and ATP concentrations

Intracellular Na$^+$, K$^+$, Cl$^-$ and ATP concentrations were calculated on the basis of intracellular water volume in cells seeded in 12-well plates. The volume of intracellular water was measured as [^{14}C]-urea available space and calculated as $V = A_c/A_m m$, where A_c was radioactivity of the cells after 30-min incubation with 2 µCi/ml [^{14}C]-urea (dpm), A_m was radioactivity of the incubation medium (dmp/µl), and m was protein content in cell lysates (mg) [66].

Transfection

Transfection of HIF-1α si-RNA (5′-AGAGGUGGAUAUGU-CUGGG-3′) and scrambled siRNA (5′-AGGAUGUGACG-GAUUGUGGTT-3′) was undertaken in the presence of Oligo-fectamine 228 (Invitrogen), as suggested by the manufacturer and described in detail elsewhere [67]. Afterwards, the cells were incubated for 24 hr under control and hypoxic conditions, as indicated above.

RNA isolatio

Total RNA was extracted from cells grown in 6-well plates with TRIzol reagent (Invitrogen) and purified with RNeasy MinElute cleanup kit (Qiagen, Valencia, CA, USA), following the manufacturers' protocols. Only RNA samples that had more than 7.0 RNA integrity number and no detectable genomic DNA contamination were considered for subsequent gene array analyses. RNA quality was assessed by 2100 Bioanalyzer (Agilent Technologies, Palo Alto, CA, USA). Microarray experiments were performed with GeneChip Human Gene 1.0 ST array (which detects 28,869 gene products) and GeneChip Rat Gene 1.0 ST array (which detects 27,342 gene products). On both arrays, each gene was represented by approximately 26 probes along the entire transcript's length (Affymetrix, Santa Clara, CA, USA). 100 ng of total RNA from each sample were processed with Ambion WT expression kit (Invitrogen), a reverse transcription method that specifically primes non-ribosomal RNA, including both poly(A) and non-poly(A) mRNA, and generates sense-strand cDNA as final product. 5.5 µg of single-stranded cDNA was fragmented and labeled by Affymetrix GeneChip WT terminal labeling kit, with 2.0 µg of the resulting cDNA hybridized on chips.

GeneChip expression analysis

RNA samples obtained from control cells and cells subjected to Na$^+$,K$^+$-ATPase inhibition with ouabain and K$^+$-free medium in 3 independent experiments were employed for GeneChip expression analysis. The controls and treatments were performed in parallel in each experiment independently from the other experiments. The entire hybridization procedure was conducted with the Affymetrix GeneChip system according to the manufacturer's recommended protocol. The hybridization results were evaluated with Affymetrix GeneChip Command Console Software. Chip quality was assessed by Affymetrix Expression Console. The data were analyzed by Partek Genomics Suite (Partek, St. Louis, MO, USA) and uploaded on the GEO repository with the accession number http://www.ncbi.nlm.nih.gov/geo/query/acc.cgi?acc=GSE61131.

The normalized data then underwent principal component analysis (PCA) [27] to identify patterns in the dataset and highlight similarities and differences among samples. Major sources of variability found within the dataset by PCA served as grouping variabilities for analysis of variance with n = 4 for each group of samples. The ensuing data were filtered to identify transcripts with statistically significant variations of expression among groups that were modulated by at least 20%, with multiple testing corrections by the false discovery rate. Calculated p-values and geometric fold changes for each probe set identifier were imported into Ingenuity Pathway Analysis (Ingenuity Systems, http://www.ingenuity.com) to ascertain networks, biological functions and their pathophysiological implications. Functional information on regulated genes was also obtained from publications in PubMed.

Real-time quantitative reverse transcription-polymerase chain reaction (RT-PCR)

RT-PCR was performed with Express SYBR GreenER qPCR Supermix kit (Invitrogen) according to the manufacturer's instructions. The reaction was carried out with a 7900 HT Fast RT – PCR system (Applied Biosystems, Foster City, CA, USA). The primers presented in Table 5 were designed with Primer3Plus online software from consensus sequences provided by Affymetrix for each gene of interest. All experiments were analyzed in duplicate. β$_2$ microglobulin mRNA expression served to normalize and compare the expression values of genes of interest. The results were quantified by the ΔΔCt method in Microsoft Excel.

Western blotting

RASMC seeded in 12-well plates were lysed on ice in 0.125 ml of buffer containing 150 mM NaCl, 1% Triton X-100, 0.1% SDS, 2 mM EDTA, 2 mM EGTA, 25 mM HEPES (pH 7.5), 10% glycerol, 1 mM NaF, 200 µM Na$_3$VO$_4$, and protease inhibitors (1 µg/ml leupeptin, 1 µg/ml aprotinin and 1 mM PMSF). The lysates were cleared off insoluble material by centrifugation at 20,000xg for 10 min, treated for 5 min at 95°C, and subjected to sodium dodecyl sulphate-polyacrylamide gel electrophoresis with 4% and 10% polyacrylamide in stacking and resolving gels, respectively. Proteins were transferred to Immobilon-P nitrocellulose membranes (Amersham, Mississauga, ON, Canada), blocked for 1 h at room temperature with 5% dry, fat-free milk dissolved in PBS and incubated overnight at 4°C with the antibodies listed below. The membranes were then treated with horseradish peroxidase-conjugated secondary antibodies and developed by enhanced chemiluminescence reaction (Amersham) in accordance with the manufacturer's instructions. Digital chemiluminescence images were taken and quantified by LAS-3000 luminescent analyzer (Fujifilm, Japan).

Chemicals

Methyl-[^{3}H]-thymidine was purchased from ICN Biomedicals, Inc. (Irvine, CA, USA). ^{22}NaCl, ^{86}RbCl, H^{36}Cl and [^{14}C]-urea were obtained from PerkinElmer (Waltham, MA, USA), Isotope (St. Petersburg, Russia) and Amersham (Montreal, QC, Canada). DEVD-AMC, DEVD-CHO and z-VAD.fmk were procured from BIOMOL Research Laboratories (Plymouth Meeting, PA, USA). Anti-HIF-1α and anti-GAPDH antibodies were sourced from Merck Millipore (Billerica, MA, USA). The remaining chemicals were supplied by Gibco BRL (Gaithersburg, MO, USA), Calbiochem (La Jolla, CA, USA), Sigma and Anachemia (Montreal, QC, Canada).

Data analysis

The main program for transcriptomic data analysis was Agilent's Genespring 7.0. Probe set intensity levels were extracted from scanned arrays by the Affymetrix GeneChip Operating Software (version 1.2) and normalized (MAS5) by all probe sets.

The probe sets were then filtered on flags (present, marginal, or absent), and expression levels were quantified. Statistically significant probe sets were identified by the false discovery rate followed by 2-way ANOVA with strain and age as major factors. Student's t-test was used for 2-group comparisons. When comparing more than 2 groups, 2-way ANOVA was employed with strain and age as the main factors, followed by Tukey's honest significant difference post-hoc test. Correlation analyses were performed with Pearson product-moment correlation coefficient (r). Null hypothesis was rejected whenever $p < 0.05$.

Author Contributions

Conceived and designed the experiments: BS SVK JT PH SNO. Performed the experiments: BS SVK JGB OAA MH. Analyzed the data: BS SVK SNO. Contributed reagents/materials/analysis tools: BS LVK SVG JT PH SNO. Wrote the paper: BS SNO.

References

1. Taylor CT (2008) Interdependent roles for hypoxia inducible factor and nuclear factor-kB in hypoxic inflammation. J.Physiol.586:4055–4059.
2. Harris AL (2002) Hypoxia - a key regulatory factor in tumour growth. Nature Rev.Cancer 2:38–47.
3. Wood IS, Perez de Heredia F, Wang B, Trayhurn P (2009) Cellular hypoxia and adipose tisue dysfunction in obesity. Proc.Nutr.Soc.68:370–377.
4. Greenstein AS, Khavandi K, Withers SB, Sonoyama K, Clancy O, et al. (2009) Local inflammation and hypoxia abolish the protective anticontractile properties of perivascular fat in obese patients. Circulation 119:1661–1670.
5. Vender RL (1994) Chronic hypoxic pulmonary hypertension. Cell biology to pathophysiology. Chest 106:236–243.
6. Castellano J, Aledo R, Sendra J, Costales P, Juan-Babot O, et al. (2011) Hypoxia stimulates low-density lipoprotein receptor-regulated protein-1 expression through hypoxia-inducible factor-1a in human vascular smooth muscle cells. Arteriosler.Thromb.Vasc.Biol.31:1411–1420.
7. Nangaku M, Eckardt KU (2007) Hypoxia and the HIF system in kidney disease. J.Mol.Med.85:1325–1330.
8. Murry CE, Jennings RB, Reimer KA (1986) Preconditioning with ischemia: a delay of lethal cell injury in ischemic myocardium. Circulation 74:1124–1136.
9. Zhao H, Ren C, Chen X, Shen J (2012) From rapid to delayed and remote postconditioning: the evolving concept of ischemic postconditioning in brain ischemia. Curr Drug Targets 13:173–187.
10. Sharp FR, Ran R, Lu A, Tang Y, Strauss KI, et al. (2004) Hypoxic preconditioning protects against ischemic brain injury. NeuroEx 1:26–35.
11. Hausenloy DJ, Yellon DM (2009) Preconditioning and postconditioning; Underlying mechanisms and clinical applications. Atherosclerosis 204:334–341.
12. Mazzatti D, Lim F-L, O'Hara A, Wood IS, Trayhurn P (2012) A microarray analysis of the hypoxia-induced modulation of gene expression in human adipocytes. Arch.Physiol.Biochem.118:112–120.
13. Lu A, Tang Y, Ran R, Clark JF, Aronow BJ, et al. (2003) Genomics of the periinfarction cortex after focal cerebral ischemia. J.Cereb.Blood Flow Met.23:786–810.
14. Kamphuis W, Dijk F, van Soest S, Bergen AAB (2007) Global gene expression profiling of ischemic preconditioning in the rat retina. Mol.Vision 13:1020–1030.
15. Tang Y, Pacary E, Freret T, Divoux D, Petit E, et al. (2006) Effect of hypoxic preconditioning on brain genomic response before and following ischemia in the adult mouse: identification of potential neuroprotective candidate for stroke. Neurobiol.Dis 21:18–28.
16. Ong LL, Oldigs JK, Kaminski A, Gerstmayer B, Piechaczek C, et al. (2010) Hypoxic/normoxic preconditioning increases endothelial differentiation potential of human bone marow CD133+ cells. Tissue End Part C Methods 16:1069–1081.
17. Manalo DJ, Rowan S, Lavoie T, Natarajan L, Kelly BD, et al. (2005) Transcription regulation of vascular endothelial cell responses to hypoxia by HIF-1. Blood 105:659–669.
18. Leonard MO, Cottell DC, Godson C, Brady HR, Taylor CT (2003) The role of HIF-1a in transcriptional regulation of the proximal tubular epithelial cell response to hypoxia. J.Biol.Chem.278:40296–40304.
19. Maxwell PH, Wiesener MS, Chang GW, Clifford SC, Vaux EC, et al. (1999) The tumor suppressor protein VHL targets hypoxia-inducible factor for oxygen-dependent proteolysis. Nature 399:271–275.
20. Kallio PJ, Pongratz I, Gradin K, McGuire J, Poellinger L (1997) Activation of hypoxia-inducible factor 1a: posttranslational regulation and conformational change by recruitment of the Arnt transcription factor. Proc.Natl.Acad.Sci.USA 94:5667–5672.
21. Semenza GL, Jiang BH, leung SW, Passantino R, Concordet JP, et al. (1996) Hypoxia response elements in the aldolase A, enolase 1, and lactate dehydrogenase A gene promoters contain essentia binding sites for hypoxia-inducible factor 1. J.Biol.Chem 271:32529–32537.
22. Ke Q, Costa M (2006) Hypoxia-inducible factor-1 (HIF-1). Mol.Pharmacol.70:1469–1480.
23. Williams RS, Benjamin IJ (2000) Protective responses in the ischemic myocardium. J.Clin.Invest.106:813–818.
24. Coulon V, Blanchard J-M (2001) Flux calciques et expression génique. Médicine Sciences 17:969–978.
25. Lee J-M, Grabb MC, Zipfel GJ, Choi DW (2000) Brain tissue responses to ischemia. J.Clin.Invest.106:723–731.
26. Koltsova SV, Trushina Y, Haloui M, Akimova OA, Tremblay J, et al. (2012) Ubiquitous [Na+]i/[K+]i-sensitive transcriptome in mammalian cells: evidence for Ca2+i-independent excitation-transcription coupling. PLoS One 7:e38032.
27. Pearson K (1901) On lines and planes of closest fit to systems of points in space. Philos.Mag.2:559–572.
28. Schoner W, Scheiner-Bobis G (2007) Endogenous and exogenous cardiac glycosides: their role in hypertension, salt metabolism, and cell growth. Am.J.Physiol.Cell Physiol.293:C509–C536.
29. Liu J, Xie Z (2010) The sodium pump and cardiotonic steroids-induced signal transduction protein kinases and calcium-signaling microdomain in regulation of transporter traficking. Biochim.Biophys.Acta 1802:1237–1245.
30. Bezanilla F (2008) How membrane proteins sense voltage. Nat.Rev.Mol.Cell Biol 9:323–332.
31. Okamura Y, Dizon JE (2011) Voltage-sensing phosphatase: its molecular relationship with PTEN. Physiology 26:6–13.
32. Tupler R, Perini G, Green MR (2001) Expresing the human genome. Nature 409:832–833.
33. Cummins EP, Taylor CT (2005) Hypoxia-responsive transcription factors. Pfluger Arch.- Eur.J.Physiol 450:363–371.
34. Phillis JW, Horrocks LA, Farooqui AA (2006) Cyclooxygenases, lypoxygenases, and epoxygenases in CNS: their role and involvement in neurological disorders. Brain Res 52:201–243.
35. Yang DH, Hsu CF, Lin CY, Guo JY, Yu WC, et al. (2013) Kruppel-like factor 10 upregulates the expression of cyclooxygenase 1 and further modulates angiogenesis in endothelial cell and platelet aggregation in gene-deficient mice. Int.J.Biochem.Cell Biol 45:419–428.
36. Kim B-J, Kim H, Cho E-J, Youn H-D (2008) Nur77 upregulates HIF-a by inhibiting pVHL-mediated degradation. Exp.Mol.Med 40:71–83.
37. Kobayashi T, Terada Y, Kuwana H, Tanaka H, Okada T, et al. (2008) Expression and fucntion of the Delta-1/NOtch-2/Hes-1 pathway during experimental acute kidney injury. Kidney Int 73:1240–1250.
38. Hamet P, Tremblay J (2006) Genetics of the sleep-wake cycle and its disorders. Metabolism Clin.Exp 55:S7–S12.
39. Koyanagi S, Kuramoto Y, Nakagawa H, Aramaki H, Ohdo S, et al. (2003) A molecular mechanism regulating circadian expression of vascular endothelial growth factor in tumor cells. Cancer Res 63:7277–7283.
40. Eckle T, Hartmann K, Bonney S, Reithel S, Mittelbronn M, et al. (2012) Adora2b-elicited Per2 stabilization promotes a HIF-dependent metabolic switch critical for myocardial adaptation to ischemia. Nature Med 18:774–782.
41. Zhang H, Qian DZ, Tan YS, Lee K, Gao P, et al. (2008) Digoxin and other cardiac glycosides inhibit HIF-1a synthesis and block tumor growth. Proc.Natl.Acad.Sci.USA 105:19579–19586.
42. Zuloaga KL, Gonzales RJ (2011) Dihydrotestosterone attenuates hypoxia inducible factor-1a and cyclooxygenase-2 in cerebral arteries during hypoxia with glucose deprivation. Am.J.Physiol.Heart Circ.Physiol 301:H1882–H1890.
43. Camacho M, Rodriguez C, Guadall A, Alcolea S, Orriols M, et al. (2011) Hypoxia upregulates PGI-synthase and increases PGI2 release in human vascular cells exposed to inflammatory stimuli. J.Lipid Res 52:720–731.
44. Zhang N, Walker MK (2007) Crosstalk between the aryl hydrocarbon receptor and hypoxia on the constitutive expression of cytochrome P4501A1 mRNA. Cardiovasc. Toxicol 7:282–290.
45. Liu Y, Cox RS, Morita T, Kourembanas S (1995) Hypoxia regulates vascular endothelial growth factor gene expression in endothelial cells: identification of a 5 prime enhancer. Circ.Res 77:638–643.
46. Hu J, Disher DJ, Bishopric NH, Webster KA (1998) Hypoxia regulates expression of the endothelin-1 gene through a proximal hypoxia-inducible factor-1 binding site on the antisense strand. Biochem. Biophys.Res.Commun 245:894–899.
47. Chakravarty A, Carlson JM, Khetani RS, Gross RH (2007) A novel ensemble learning method for de novo computational identification of DNA binding sites. BMC Bioinformatics 8:249.
48. Murphy E, Eisner DA (2009) Regulation of intracellular and mitochondrial sodium in health and disease. Circ.Res 104:292–303.
49. Wenger RH, Stiehl DP, Camenisch G (2005) Integration of oxygen signaling at the consensus HRE. Sci.STKE 306:re12.

50. Reyes H, Reisz-Porszasz S, Hankinson O (1992) Identification of the Ah receptor nuclear translocation protein Arnt as a component of the DNA binding form of the Ah receptor. Science 256:1193–1195.
51. Schultz MA, Timmermans L, Godschalk RW, Theys J, Wouters BG, et al. (2010) Diminished carcinogen detoxification is a novel mechanism for hypoxia-inducible factor 1-mediated genetic instability. J.Biol.Chem 285:14558–14564.
52. Chen R, Castranova V, Shi X, Demers LM (1999) New insights into the role of nuclear factor-kB, a ubiquitous transcription factor in the initiation of deseases. Clin.Chem 45:7–17.
53. Alarcon R, Koumenus C, Geyer RK, Maki CG, Giaccia AJ (1999) Hypoxia induces p53 accumulation through MDM2 down-regulation and inhibition of E6-mediated degradation. Cancer Res 59:6046–6051.
54. Ahn Y-L, Kim H, Lim H, Lee M, Kang Y, et al. (2012) AMP-activated protein kinase: implications on ischemic diseases. BMB reports 45:489–495.
55. Yan S-F, Lu J, Zou YS, Soh-Won J, Cohen DM, et al. (1999) Hypoxia-associated induction of early growth response-1 gene expression. J.Biol.Chem 274:15030–15040.
56. Taurin S, Dulin NO, Pchejetski D, Grygorczyk R, Tremblay J, et al. (2002) c-Fos expression in ouabain-treated vascular smooth muscle cells from rat aorta: evidence for an intracellular-sodium-mediated, calcium-independent mechanism. J.Physiol 543:835–847.
57. McDonald TF, Pelzer S, Trautwein W, Pelzer DJ (1994) Regulation and modulation of calcium channels in cardiac, skeletal, and smooth muscle cells. Physiol.Rev 74:365–512.
58. Blaustein MP, Lederer WJ (1999) Sodium/calcium exchange: its physiological implications. Physiol.Rev 79:763–854.
59. Alberini CA (2009) Transcription factors in long-term memory and synaptic plasticity. Physiol.Rev 89:121–145.
60. Orlov SN, Aksentsev SL, Kotelevtsev SV (2005) Extracellular calcium is required for the maintenance of plasma membrane integrity in nucleated cells. Cell Calcium 38:53–57
61. Johnson AB, Denko N, Barton MC (2008) Hypoxia induces a novel signature of chromatin modifications and global repression of transcription. Mutat.Res 640:174–179
62. Lanctôt C, Cheutin T, Gremer M, Cavalli G, Cremer T (2007) Dynamic genome architecture in the nuclear space: regulation of gene expression in three dimensions. Nature Rev.Genet 8:104–115.
63. Gibcus JH, Dekker J (2013) The hierarchy of the 3D genome. Mol.Cell 49:773–782.
64. Akimova OA, Bagrov AY, Lopina OD, Kamernitsky AV, Tremblay J, et al. (2005) Cardiotonic steroids differentially affect intracellular Na^+ and $[Na^+]i/[K^+]i$-independent signaling in C7-MDCK cells. J.Biol.Chem 280:832-839.
65. Akimova OA, Grygorczyk A, Bundey RA, Bourcier N, Gekle M, et al. (2006) Transient activation and delayed inhibition of Na+,K+,Cl- cotransport in ATP-treated C11-MDCK cells involve distinct P2Y receptor subtypes and signaling mechanisms. J.Biol.Chem 281:31317–31325.
66. Orlov SN, Tremblay J, Hamet P (1996) Cell volume in vascular smooth muscle is regulated by bumetanide-sensitive ion transport. Am.J.Physiol 270:C1388–C1397.
67. Egger M, Schgoer W, Beer AGE, Jeschke J, Leierer J, et al. (2007) Hypoxia up-regulates the angiogenic cytokine secretoneurin via HIF-1α and basic FGF-dependent pathway in muscle cells. FASEB J 21:2906–2917.

20